USGS
science for a changing world

Preliminary Observations of Voluminous Ice-Rich and Water-Rich Lahars Generated During the 2009 Eruption of Redoubt Volcano, Alaska

Open-File Report 2012-1078

U.S. Department of the Interior
U.S. Geological Survey

Preliminary Observations of Voluminous Ice-Rich and Water-Rich Lahars Generated During the 2009 Eruption of Redoubt Volcano, Alaska

By Christopher F. Waythomas, Thomas C. Pierson, Jon J. Major, and William E. Scott

Open-File Report 2012-1078

U.S. Department of the Interior
U.S. Geological Survey

U.S. Department of the Interior
KEN SALAZAR, Secretary

U.S. Geological Survey
Marcia K. McNutt, Director

U.S. Geological Survey, Reston, Virginia: 2012

Suggested citation:
Waythomas, C.F., Pierson, T.C., Major, J.J., and Scott, W.E., 2012, Preliminary observations of voluminous ice-rich and water-rich lahars generated during the 2009 eruption of Redoubt, Alaska: U.S. Geological Survey Open-File Report 2012-1078, 42 p.

Contents

Figures

Tables

Conversion Factors and Datums

Conversion Factors

SI to Inch/Pound

Multiply	By	To obtain
	Length	
centimeter (cm)	0.3937	inch (in.)
millimeter (mm)	0.03937	inch (in.)
meter (m)	3.281	foot (ft)
meter (m)	1.094	yard (yd)
kilometer (km)	0.6214	mile (mi)
kilometer (km)	0.5400	mile, nautical (nmi)
	Area	
square meter (m^2)	0.0002471	acre
square meter (m^2)	10.76	square foot (ft^2)
square centimeter (cm^2)	0.1550	square inch (ft^2)
square kilometer (km^2)	0.3861	square mile (mi^2)
	Volume	
cubic centimeter (cm^3)	0.06102	cubic inch (in^3)
cubic kilometer (km^3)	0.2399	cubic mile (mi^3)
cubic meter (m^3)	6.290	barrel (petroleum, 1 barrel = 42 gal)
cubic meter (m^3)	264.2	gallon (gal)
cubic meter (m^3)	0.0002642	million gallons (Mgal)
cubic meter (m^3)	35.31	cubic foot (ft^3)
cubic meter (m^3)	1.308	cubic yard (yd^3)
cubic meter (m^3)	0.0008107	acre-foot (acre-ft)
	Flow rate	
cubic meter per second (m^3/s)	70.07	acre-foot per day (acre-ft/d)
cubic meter per second (m^3/s)	35.31	cubic foot per second (ft^3/s)
meter per second (m/s)	3.281	foot per second (ft/s)
meter per minute (m/min)	3.281	foot per minute (ft/min)
kilometer per hour (km/h)	0.6214	mile per hour (mi/h)
	Mass	
gram (g)	0.03527	ounce, avoirdupois (oz)
kilogram (kg)	2.205	pound avoirdupois (lb)
	Density	
kilogram per cubic meter (kg/m^3)	0.06242	pound per cubic foot (lb/ft^3)
gram per cubic centimeter (g/cm^3)	62.4220	pound per cubic foot (lb/ft^3)

Temperature in degrees Celsius (°C) may be converted to degrees Fahrenheit (°F) as follows:
°F=(1.8×°C)+32
Temperature in degrees Fahrenheit (°F) may be converted to degrees Celsius (°C) as follows:
°C=(°F-32)/1.8

Datums

Vertical coordinate information is referenced to the insert datum name (and abbreviation) here, for instance, "North American Vertical Datum of 1988 (NAVD 88)"
Horizontal coordinate information is referenced to the insert datum name (and abbreviation) here, for instance, "North American Datum of 1983 (NAD 83)"
Altitude, as used in this report, refers to distance above the vertical datum.

Preliminary Observations of Voluminous Ice-Rich and Water-Rich Lahars Generated During the 2009 Eruption of Redoubt Volcano, Alaska

By Christopher F. Waythomas, Thomas C. Pierson, Jon J. Major, and William E. Scott

Abstract

Redoubt Volcano in south-central Alaska began erupting on March 15, 2009, and by April 4, 2009, had produced at least 20 explosive events that generated plumes of ash and lahars. The 3,108-m high, snow- and -ice-clad stratovolcano has an ice-filled summit crater that is breached to the north. The volcano supports about 4 km^3 of ice and snow and about 1 km^3 of this makes up the Drift glacier on the northern side of the volcano. Explosive eruptions between March 22 and April 4, which included the destruction of at least two lava domes, triggered significant lahars in the Drift River valley on March 23 and April 4 and several smaller lahars between March 24 and March 31. High-flow marks, character of deposits, areas of inundation, and estimates of flow velocity revealed that the lahars on March 23 and April 4 were the largest of the eruption. In the 2-km-wide upper Drift River valley, average flow depths were about 3–5 m. Average peak-flow velocities were likely between 10 and 15 ms^{-1}, and peak discharges were on the order of 10^4–10^5 m^3s^{-1}. The area inundated by lahars on March 23 was at least 100 km^2 and on April 4 about 125 km^2. The lahars emplaced on March 23 and April 4 had volumes on the order of 10^7–10^8 m^3 and were similar in size to the largest lahar of the 1989–90 eruption. The March 23 lahars were primarily flowing slurries of snow and ice entrained from the Drift glacier and seasonal snow and tabular blocks of river ice from the Drift River valley. Only a single, undifferentiated deposit up to 5 m thick was found and contained about 80–95 percent of poorly sorted, massive to imbricate assemblages of snow and ice. The deposit was frozen soon after it was emplaced and later eroded and buried by the April 4 lahar. The lahar of April 4, in contrast, was primarily a hyperconcentrated flow, as interpreted from 1- to 6-m thick deposits of massive to horizontally stratified sand-to-fine-gravel. Rock material in the April 4 lahar deposit is predominantly juvenile andesite. We infer that the lahars generated on March 23 were initiated by a rapid succession of vent-clearing explosions that blasted through about 50–100 m of crater-filling glacier ice and snow, producing a voluminous release of meltwater from the Drift glacier. The resulting flood eroded and entrained snow, fragments of glacier and river ice, and liquid water along its flow path. Small-volume pyroclastic flows, possibly associated with destruction of a small dome or minor eruption-column collapses, may have contributed additional meltwater to the lahar. Meltwater generated by subglacial hydrothermal activity and stored beneath the Drift glacier may have been ejected or released rapidly as well. The April 4 lahar was initiated when hot dome-collapse pyroclastic flows entrained and swiftly melted snow and ice, and incorporated additional rock debris from the Drift glacier. The peak discharge of the April 4 lahar was in the range of 60,000–160,000 m^3s^{-1}. For comparison, the largest lahar of the 1989–90 eruption had a peak discharge of about 80,000 m^3s^{-1}. Lahars generated by the 2009 eruption led to significant channel aggradation in the lower Drift River valley and caused extensive inundation at an oil storage and transfer facility located there. The April 4, 2009, lahar was 6–30 times larger than the largest meteorological floods known or estimated in the Drift River drainage.

Introduction

Setting

Eruptions at Alaskan volcanoes almost always involve snow and ice, and lahars are a common product of eruptive activity regardless of eruption magnitude or duration. Redoubt Volcano is an historically active, andesite to dacite stratocone in the Cook Inlet region of Alaska (fig. 1) that experienced its most recent eruption in March–July 2009 (Schaefer, 2012). Prior to the start of the 2009 eruption, the volcano supported about 4 km^3 of glacier ice and perennial snow (Trabant and Hawkins, 1997), about 1 km^3 of which formed the Drift glacier on the northern flank of the volcano (fig. 1). Downstream of the Drift glacier, the Drift River flows 35 km eastward to Cook Inlet. The Drift River has a wide braided channel that occupies a 1.5- to 2.5-km-wide valley in its bedrock-confined upper and middle reaches. The lower 10 km of the valley is less confined and broadens over a narrow coastal plain, where it is as much as 9 km wide and includes a number of distributary channels (fig. 1).

Redoubt Volcano has erupted more than 50 times in the past 10,000 years and four times since 1900 (Begét and Nye, 1994; Till and others, 1994; Schiff and others, 2010). All known historical eruptive activity, and probably several prehistoric eruptions, have occurred from vents within the breached, 1×2 km, ice-filled summit crater at the head of the Drift glacier (fig. 2). During the three eruptions of the past 46 years (1966–68, 1989–90, 2009), each produced multiple lahars in the Drift River valley (Sturm and others, 1986; Dorava and Meyer, 1994; Schaefer, 2012). Lahars associated with these recent eruptions have inundated significant parts of the lower Drift River and associated distributary channels. The lahars produced during the 1989–90 and 2009 eruptions have posed a significant hazard to the oil-production infrastructure located near the mouth of the Drift River—both to pipelines buried beneath the river and to the Drift River Marine Terminal (DRMT), an oil storage and transfer facility (fig. 1).

Redoubt Volcano began erupting in 2009 with a small phreatic explosion on March 15. A series of 19 discrete explosive events from late evening on March 22 (AKDT) through April 4 produced at least five limited run-out pyroclastic flows and at least 20 lahars (fig. 3) before the eruption transitioned to its final effusive phase that ended about July 1 (Schaefer, 2012). Almost all lahars were triggered by rapid melt of ice and snow that occurred within minutes of explosions from the vent. The largest lahars occurred on March 23, March 26, and April 4. The lahars generated on March 23 were ice rich and were distinctly different in character from the more water-rich lahars of March 26 and April 4. The lahars produced on March 23 and April 4 overtopped and flowed around protective levees at the DRMT, depositing mud, vegetation, and ice, and severely impacting operations but not resulting in any oil spills (Schaefer, 2012). In this paper, we characterize the largest flows, estimate their peak discharges and volumes, discuss their contrasting compositions and origins, and provide an updated context for future lahar hazards in the Drift River valley.

Lahars at Snow- and Ice-Clad Volcanoes

Mass flows composed of high-concentration mixtures of sediment, ice, and water are expected consequences of eruptions at snow- and ice-clad volcanoes (Major and Newhall, 1989). Such flows, known as lahars, typically are classified as one of two types according to their proportions of solids and water: debris flows (about 50–75 percent solids by volume) and hyperconcentrated flows (about 10–50 percent solids by volume) (Vallance, 2000; Pierson, 2005). Documented lahars having solid components that are dominated by ice fragments (and are thus ice-rich lahars; also known as ice-slurry flows, snow-slurry lahars, ice-diamict flows, and mixed avalanches) typically have volumes of 10^7 m^3 or less and runout distances no greater than about 15 km (Pierson and Janda, 1994; Waitt and others, 1994; Cronin

and others, 1996; Kilgour and others, 2010). More commonly, lahars generated by explosive eruptions at snow- and ice-clad volcanoes are water-saturated, high-concentration mixtures of mostly rock fragments, water, and minor amounts of ice. Such lahars typically are initiated by the dynamic interaction of hot pyroclastic debris with snow and ice (Major and Newhall, 1989; Walder, 2000a, 2000b). In contrast to ice-rich flows, ice-poor lahars can have flow volumes as much as 10^8–10^9 m^3 and runout distances in excess of 100 km (Pierson and others, 1990; Dorava and Meyer, 1994; Mothes and others, 1998; Major and others, 2005).

Past Lahars at Redoubt Volcano

Extensive inundation of the Drift River valley by large to very large[1] lahars is common during explosive magmatic eruptions of Redoubt. Such lahars were documented during the previous two eruptions in 1966–68 and 1989–90 (Sturm and others, 1986; Dorava and Meyer, 1994). On January 25, 1966, an explosive event generated a lahar of unknown volume but was assumed to be large to very large, which probably was triggered by a pyroclastic flow. This lahar inundated the lower Drift River valley (extent of inundation not known), transporting blocks of ice many meters in diameter and forcing the evacuation of a survey crew working in the area of the yet to be constructed DRMT (Anchorage Daily News, XIX, no. 149, 1966). A second lahar was generated on February 9, 1966, but apparently contained little or no ice (Riehle, and others, 1981). Both lahars had local flow depths of at least 4–6 m, but their volumes and peak discharges are unknown.

During the 1989–90 eruption, at least 18 lahars were generated by vigorous vent explosions or pyroclastic flows associated with collapses of lava domes (Brantley, 1990). Three of these lahars were large enough to threaten or cause damage to the DRMT (Dorava and Meyer, 1994). The December 15, 1989, flow had a peak stage about 3 m below the elevation of an earthen levee surrounding the DRMT but did not impinge on the levee directly. The January 2, 1990, lahar flowed around the terminal's protective levees on the upstream side, inundating buildings, roads, and the facility runway on the downstream side; the lahar came within 0.2 m of overtopping the containment levees surrounding individual oil tanks (Brantley, 1990; Dorava and Meyer, 1994). This lahar, the largest of the eruption, commenced as a meltwater flood of about 25 million m^3 (Dorava and Meyer, 1994; Trabant, and others, 1994), which then entrained tephra, pyroclastic debris, supraglacial debris, and alluvium to transform to a debris flow having a volume on the order of 10^7–10^8 m^3 (Gardner and others, 1994). The estimated peak discharge for this debris flow was 16,000–80,000 m^3s^{-1} in the upper Drift River valley about 2.5 km downstream of the terminus of the Drift glacier (Dorava and Meyer, 1994). The lahar transported ice blocks up to 8 m in diameter to Cook Inlet and inundated the Drift River valley to an extent comparable to the largest lahars of the 2009 eruption. The February 15, 1990, lahar was smaller and more dilute than the January 2 flow, but the February flow also flooded the DRMT and breached one of the oil tank containment levees (Dorava and Meyer, 1994).

The sediment delivered to the lower Drift River valley by the 1990 lahars aggraded the valley floor and promoted rapid and unpredictable lateral shifts in the position of the active channel. During July–August 1990, the Drift River avulsed northward from its main channel into adjacent Montana Bill Creek (fig. 1), which thereafter conveyed an estimated 70–90 percent of the flow of Drift River. This resulted in significant scour of the bed of lower Montana Bill Creek, exposing the buried oil pipeline that feeds the DRMT (Dorava and Meyer, 1994).

[1] "Large" lahars have near-source peak discharges of 10^3–10^4 m^3s^{-1}; "very large" lahars have near-source peak discharges of 10^4–10^6 $m^3s^{-1}m^3$ (Pierson, 1998). Corresponding volumes from the 10-fold size classification of Jakob (2005) are roughly 10^5–10^6 m^3 for large lahars and 10^6–10^8 m^3 for very large lahars (Jakob, 2005).

Eruption Effects on the Drift Glacier in 2009

The 2009 eruption began on March 15, 2009, and included at least 20 explosive events through April 4 (Schaefer, 2012). Prior to the 2009 eruption, up to 100 m of ice and snow filled the volcano's breached summit crater and canyon below (fig. 2) and was available to mobilize lahars. Most of this was removed by the 1989–90 eruption, but occasional observations by Alaska Volcano Observatory scientists showed it was replaced over about the next 10 years, similar to glacier growth following the eruption in 1966–68 (Sturm and others, 1986). Increased heat flow and fumarolic activity during the 8 months of precursory unrest prior to the 2009 eruption (Schaefer, 2012) caused some melting of ice and the formation of collapse features by late February 2009. Our mapping of ice-melt features on satellite imagery, aerial observations, and estimates of ice thickness suggest that $3–7\times10^6$ m^3 of glacier ice and snow was lost from the crater and the upper Drift glacier between late July 2008 and March 20, 2009.

At the time of the eruption, the upper part of the Drift glacier occupied a narrow, steep, bedrock gorge downslope of the crater breach. The gorge not only restricted glacier width but also funneled pyroclastic flows and meltwater floods originating at the crater. Such topographic focusing of hot flows enhances ice scour and melting and appears to be a highly efficient mechanism for meltwater generation.

At least five major vent-clearing explosions on March 23 (Schaefer, 2012) erupted through glacier ice and snow, destroyed a small lava dome (and possibly all or part of the last 1990 lava dome), and produced a funnel-shaped explosion crater within the larger, ice-filled summit crater. Explosive events mentioned throughout the paper, and shown in figure 3, are the main, named events associated with explosion signals (Schaefer, 2012). Reanalysis of seismic data identified several additional less vigorous explosive events, but these were not numbered sequentially. Proximal tephra deposits from explosive event 5, the last major explosive event on March 23 (fig. 3), contained significant amounts of angular pebble-sized ice particles (Schaefer, 2012), indicating that during the opening phase of the eruption glacier ice was explosively fragmented and ejected from the vent area. During this explosion, some amount of ice was likely melted as well. Aerial observations of the Drift glacier in the gorge area downslope of the vent, made on the afternoon of March 23, indicated that the glacier, as much as 100 m thick, had been locally scoured to bedrock. Although no pyroclastic-flow deposits were identified, the degree of ice erosion and the amount of meltwater in the ensuing lahar suggest that small, limited-runout pyroclastic flows may have formed. Meltwater generated by subglacial hydrothermal activity and stored in the summit crater beneath the Drift glacier also may have been released during the initial phase of the eruption, but any water stored there was of limited volume due to geometric constraints of the crater and the prevalence of ice collapse features indicating release, rather than storage, of meltwater.

Analysis of a satellite image obtained on March 26, the first clear day after March 23, showed that about $0.5–1.5\times10^8$ m^3 of ice and snow had been removed from the upper Drift glacier, including part of the summit crater (table 1). This value reflects the total ice loss caused by explosive events 1–8 (fig. 3), much of which probably occurred during explosive events 4–6, which were major events and associated with significant lahars. Another source of water for lahars was river ice and snow in the Drift River valley, where the snow depth was estimated by Alaska Volcano Observatory scientists to be up to 2 m in some areas. Explosive events 9–18 from March 27–29 caused further melting of the Drift glacier, but the extent of ice loss during this period could not be determined, because clouds continuously obscured the volcano and much of the Drift River valley. A strong explosion and a major collapse of a growing lava dome at 13:58 UTC on April 4 (event 19) removed another $0.5–1.0\times10^8$ m^3 of ice from the Drift glacier. A pyroclastic flow from the dome collapse caused significant scour of the glacier surface and initiated a very large lahar on April 4.

Total ice volume lost during 2009 and 1989–90 eruptions was of the same order of magnitude. Ice loss during 2009 was about 1–2.5×10^8 m^3 or about 10–25 percent of the total glacier volume (table 1). Most of the ice loss occurred on the upper Drift glacier between an altitude of about 700 and 2,000 m. The amount of the Drift glacier removed during the 1989–90 eruption was 29×10^8 m^3 ±5 percent (Trabant and Hawkins, 1997), or about 30 percent of the total.

2009 Eruption and Lahars

Explosive events between March 23 and April 4 destroyed at least two lava domes and triggered four large to very large lahars in the Drift River valley—two on March 23, one on March 26, and one on April 4—and several smaller lahars between March 24 and March 30 (fig. 3, table 2). The four largest lahars inundated most of the upper and middle reaches of the Drift River valley and a broad area of its lower reach. The lahars of March 23 and April 4 overtopped and flowed around protective levees at the DRMT, depositing mud and debris that severely impacted operations at the facility, but did not result in any oil spills.

Most of the lahars triggered by the 2009 eruption were recognized on the basis of seismic data from stations DFR and RDE along the Drift River valley (fig. 1). No lahars were observed directly, but limited aerial observations and remote camera images provided confirmation of several lahar occurrences, usually within hours of emplacement. Lahar signals were identified during visual examination of seismic data, and they commonly appeared soon after individual explosive events as sustained seismic activity having broadly distributed energy spectra and gradually decreasing seismic coda (fig. 4) (H. Buurman, University of Alaska-Fairbanks, written commun., 2012). Throughout the 2009 eruption, the onset of a lahar was defined as the time of minimum signal-to-noise ratio (SNR) between the peak of an explosion signal and a sustained lahar signal. The end of a lahar was defined as the time when the SNR decreased to less than 2. The difference between the start and end times provides the seismic duration of a lahar. Uncertainties about the character of the seismic source and the propagation path of seismic energy between the lahar source and the seismic station make it difficult to infer anything specific about the flow characteristics of lahars detected seismically.

Lahars of March 23

Eight explosions within 7 hours on March 23 produced three seismically detectable lahars in the upper Drift River valley, at least one of which reached the DRMT (fig. 3). The first lahar of the eruption (lahar 1) occurred just after midnight local time (08:40 UTC) March 23 (fig. 3). The three lahars detected seismically during this initial period of explosive activity (lahars 1, 2, and 3; fig. 3) correlate with explosive events 3, 4, and 5, respectively, of the eruption sequence. It is not known if any small lahars were produced during explosive events 1 and 2, but no flowage signals were detected at stations DFR and RDE immediately following these events. Lahars 1 and 2 occurred at night and were not observed.

Lahar 2 had the longest seismic duration (111 minutes at both stations DFR and RDE) of all of the lahars and among the highest maximum seismic amplitudes of the largest lahars (fig. 5), suggesting a substantial, energetic flow. This lahar appears to have resulted from two closely spaced explosive events at 09:38 UTC and 09:48 UTC on March 23 (fig. 3).

Lahar 3 was detected seismically at 12:38 UTC and had a seismic duration of about 47 minutes and the second largest maximum seismic amplitude of all of the lahars emplaced during the eruption (fig. 5). Oblique aerial photographs taken during a late afternoon reconnaissance flight on March 23 show a fresh but partially snow-covered lahar deposit that is wider and more extensive in the upper valley than a subsequent cross-cutting lahar deposit that had no snow cover (fig. 6A). The snow-covered deposit probably was produced by lahar 2, and the deposit lacking snow cover was produced by lahar 3. In the lower valley, the crosscutting relations of these initial lahars were not evident in aerial imagery.

A lahar large enough to seem threatening to DRMT personnel reached the facility between about 13:30–14:00 UTC (05:30–06:00 AKDT), and afterwards, all personnel were evacuated (Schaefer, 2012). If this was lahar 2 triggered by explosive event 4 at 09:38 UTC, travel time would have been about 4–4.5 hours and its average flow-front velocity (from summit crater vent to DRMT) would have been about 3 ms^{-1} (flow path length = 44 km). If the flow was lahar 3, which was triggered by explosive event 5 at 12:30 UTC, the travel time would have been 1.5 hours and average flow-front velocity would have been about 8–12 ms^{-1}. Empirical travel time curves given in Pierson (1998) indicate that average travel times for large lahars to points 40 km from source are in the range of 1.5–3 hours, and very large lahars are in the range of about 0.5–1.5 hours. These values suggest that lahar 3 was the flow observed at the DRMT early that morning. We cannot confirm that lahar 2 did not reach the facility; it likely did, but was not observed by personnel. The ice content of lahars 2 and 3 and the frozen ice and snow covered valley floor the lahars overrode likely resulted in unsteady, pulsatory flows. Such factors would have reduced the fluidity of the lahars, thereby increasing the uncertainty of travel times relative to other lahars and possibly allowing lahars generated hours apart to merge.

Observations made during the March 23 reconnaissance flight indicated extensive lahar inundation throughout the Drift River valley (fig. 6A), particularly in the area south of the DRMT in the Rust Slough-Cannery Creek drainage (fig. 6B). The oil terminal had been surrounded and partially inundated by the lahar, and the runway at the facility was completely covered with sediment, ice, trees, vegetation, and standing water. Material transported by the lahar was deposited against the protective levees that surrounded the DRMT tank farm at the west (upstream) end of the facility. The level of sediment and debris reached to the top of the levees and in a few places muddy water overtopped the levee crest that stood about 2 m above the flood plain prior to March 23 (fig. 6B). A few of the service roads within the facility were inundated and covered by mud, water, and meter-size clasts of ice that were emplaced by back-flow up several roads between the runway and the tanks. Along the middle and upper parts of the Drift River, trunks of mature trees were stripped of bark (probably by ice blocks entrained in the flow) to a height of several meters above the top of the lahar deposit and prominent mud and debris lines were evident along the channel (fig. 6C). In many areas along the valley margin, deposits consisting chiefly of interlocking tabular ice blocks and subangular to rounded ice cobbles were emplaced and then frozen, preserving the ice-rich deposit fabric (figs. 6D, 6E, 6F). Deposits consisting of an ice-grain matrix supporting cobble- to boulder-size clasts of ice (figs. 6G, 6H) also were preserved in various locations throughout the valley.

The main channel of the Drift River along the northern side of the DRMT was plugged with sediment and logs, which caused the active channel of the Drift River to shift southward into the Rust Slough-Cannery Creek drainage (fig. 7). Farther upstream in the confined, 1.5–2-km-wide middle Drift River valley, prominent sediment benches, mud lines, and the upper limit of snow erosion indicated local flow depths of 6–8 m above the valley floor. At Dumbbell Hill, a bedrock knob in the Drift River channel about 3 km downstream of the terminus of the Drift glacier (fig. 1), ripped up clasts of frozen sediment were emplaced on the upstream (west) side of the hill nearly reaching an equipment house on the top of the hill about 15 m above the valley floor. In this area, large clasts of ice, many meters in length, were scattered about on the valley floor. Unlike many of the 1989–90 lahar deposits, no steaming clasts or boulders of juvenile rock were observed on the surface of the March 23 deposit.

Lahars of March 24–30

At least 16 lahars were detected seismically, observed in time-lapse camera images, or both, from March 24 to March 30 (table 2, fig. 3). Lahars on March 24–27 had seismic durations and amplitudes approaching or, in some cases, exceeding those associated with lahars 2 and 3 on March 23 (fig. 5). Lahar 6 on March 26 was one of the four largest lahars of the eruption, based on relatively extensive inundation of the valley documented from satellite imagery and observations made during helicopter overflights (figs. 8 and 9). Limited photographic evidence, however, suggests that most flows of this time period were watery and had low peak discharges.

Data and imagery from the smaller lahars recorded during this period provide the following observations:

1. A pyroclastic flow associated with explosive event 11 on March 27 swept down from the vent to the terminus of the Drift glacier (about 9 km) in about 3 minutes (average flow velocity of about 50 ms^{-1}; fig. 10A) and apparently triggered a lahar (lahar 9). The time lag between the onset of explosive activity at the vent and the appearance of the lahar at Dumbbell Hill (13 km downstream of vent) was about 17 min (fig. 10), but, owing to uncertainty about the timing and location of lahar formation, we cannot meaningfully estimate lahar velocity. The lahar appears to have inundated a part of the upper Drift River valley (fig. 10B), but its downstream extent is not known.
2. Some small lahars were not associated with seismically detected explosion signals (lahars 15, 18, 19; fig. 3). The small lahars possibly were caused by release of meltwater from the glacier or local damming of channels on the glacier as inferred in 1989–90 (Trabant and others, 1994).
3. Some small lahars or floods were warm, and their deposits were steaming temporarily (fig. 10B).
4. Not all explosions from the vent generated floods or lahars (fig. 3).

Lahar of April 4

Lahar 20 on April 4 was detected seismically, observed in time-lapse camera and satellite images, and was the most extensive lahar of the 2009 eruption. This lahar followed a strong explosive event (event 19) at 13:58 UTC, which involved a major failure of the lava dome that had grown at the mouth of the summit crater. What appears to be the front of the April 4 lahar reaching Dumbbell Hill (13 km from the vent) was photographed by time-lapse camera at 14:11 UTC (fig. 11), 13 minutes after explosive event 19 began. The lahar was detected for about 80 minutes at station DFR and about 1 hour and 50 minutes at station RDE. This lahar also had the largest maximum seismic amplitude of all lahars at station RDE and the second largest maximum seismic amplitude on station DFR, exceeded only by lahar 3 on March 23 (fig. 5).

An overflight on the afternoon of April 4 indicated that the lahar had completely inundated the upper and middle reaches of the Drift River valley and about 80 percent of the unconfined lower reach of the valley near the DRMT (figs. 12 and 13). Partial inundation of the DRMT caused some flooding of facilities, roads, and buildings, and again covered the airstrip with muddy sediment, trees, blocks of ice, and other debris. The lahar surrounded the oil storage area and reached the top of, but did not breach, the containment levees. Minor flow and wet ground were observed along the main channel of the Drift River indicating that partial flow was reestablished temporarily in the mainstem of the channel north of the DRMT. As the lahar waned, the active channel was confined within the channels south of the DRMT where it remained as of autumn 2011.

Although many blocks of glacier and river ice 2–5 m in length were observed on the surface of the April 4 lahar deposit as far downstream as the DRMT, internally the deposit was mostly devoid of ice. Thus, some ice blocks probably were reworked from the March 23 deposit. The April 4 lahar formed ubiquitous deposits of gravel, sand, and mud that completely buried prior lahar deposits, including those emplaced on March 23.

Deposit Characteristics of March 23 and April 4 Lahars

The lahars that formed on March 23 and April 4 were the largest of the 2009 eruption, and deposits produced by these flows were preserved throughout the Drift River valley, especially along the valley margins (fig. 14). Although other lahars were initiated during the eruption, no deposits attributed to them could be identified suggesting that the April 4 flow either obscured or removed all evidence of them.

Characteristics of March 23 Deposit

The maximum extent of the lahars emplaced on March 23 (fig. 7) was mapped using oblique aerial photographs obtained during reconnaissance flights on March 23 and a composite aerial image of the Drift River fan obtained on March 31, 2009, by Aerometric, Inc. By the time the March 31 imagery was collected, snow had fallen and covered parts of the deposit, making it difficult to identify the limits of the flow in some areas.

Deposits of the three March 23 lahars could not be differentiated in outcrop. Although aerial photographs of the upper Drift River valley show two apparent deposits (fig. 6A), probably associated with lahars 2 and 3, later field studies revealed only a single, undifferentiated deposit. Some outcrops may have been composites of the two deposits, but no internal boundaries were noted. We infer that the composite lahar deposit was emplaced as coarse-grained ice-slurries that froze solid soon after deposition. The deposit is underlain either by pre-eruption snowpack (corn snow with ice granules a few millimeters in diameter) or by fluvial deposits on the pre-eruption the valley floor. In some outcrops, entrainment of the underlying snowpack was clearly indicated by irregular blocks of snow preserved within the lahar deposit as well as lenses and stringers of ice- and snow-rich laharic material injected into underlying snow (fig. 6H).

The composite March 23 lahar deposit was composed almost entirely of ice fragments, ranging from sand-size grains to much larger clasts of glacier and river ice. In some locations, the ice within the deposit was clast supported and consisted predominantly of equant clasts of glacier ice up to several meters in diameter and tabular slabs of river ice several meters in length (fig. 6D). In other locations, the deposit was matrix supported with widely dispersed ice clasts (and some rock clasts) (fig. 6E, 6F). Matrix material was composed of rounded grains of clear ice (fig. 6G, 6H), estimated in the field to be largely in the range of 1–4 mm in diameter. Sand- to silt-size mineral grains, if present, were confined to the interstices between the framework ice grains and were frozen in the interstitial pore water. Rare cobble- to-pebble-size, angular to sub-angular rock clasts in the deposit were dense, non-vesicular, phenocryst-rich andesite that were either fragments of older dome rock, fragments of new magma erupted during explosive events 4 and 5, or both. Rare rounded to subrounded rock clasts derived from the underlying alluvium were present locally, and the non-ice detritus also included logs and other vegetal debris. Volumetric content of rock fragments within the lahar deposit was estimated in the field to range between 5 and 20 percent. Measured bulk density for nine matrix samples of the deposit averaged about 1.0 ± 0.1 gcm^{-3}.

The March 23 lahars inundated about 100 km^2 of the Drift River valley (fig. 7). The maximum observed thickness was 5 m, and all outcrops observed were at least 1 m thick. Aerial observations indicated that mud lines on trees near the middle of the valley, where the lahar was flowing in a relatively straight channel, were locally as much as 2–4 m above the top of the lahar deposit. In other areas where the flow was affected by bends in the channel or where deposits were pushed into channel embayments, deposits were 6–8 m above the valley floor. Mud lines on buildings and trees at the DRMT indicate a distal flow depth of about 2 m. Because of poor weather and eruption hazards, it was not possible to make systematic measurements of high-water marks associated with the March 23 lahars.

Characteristics of April 4 Deposit

The deposit of the April 4 lahar consisted almost entirely of massive to horizontally stratified, poorly sorted sand to fine gravel, 1–6 m thick where examined, and thickest in slack water areas along the valley margin (fig. 15). Locally in the upper Drift River valley, the deposit was a 1–2 m thick, massive, very poorly sorted, gray, pebble-to-cobble bearing diamict (fig. 15B), suggesting that a component of the lahar had achieved debris-flow sediment concentrations prior to transformation to hyperconcentrated flow. The matrix of the April 4 deposit contained no obvious ice fragments. Rock material in the deposit consisted of abundant cobble- to boulder-sized fragments of dense to slightly vesicular, locally prismatically jointed, medium- to light-gray juvenile andesite (fig. 15A, 15B), which we infer to have been part of the lava dome that was destroyed by the April 4 explosive episode (Coombs and others, 2012; Schaefer, 2012). The April 4 deposit also contained rare large subrounded blocks of glacier ice scoured from the Drift glacier (some as large as 200–300 m^3) and some meter-sized tabular clasts of river ice, which probably were reworked from the March 23 deposits. Glacier and river ice in the April 4 deposit was found throughout the Drift River valley, but in very low amounts relative to the March 23 deposit. The sandy April 4 deposit locally exhibited water escape structures and a capping of silt, indicative of rapid deposition and low deposit permeability (fig. 15D)—characteristics of deposition by hyperconcentrated flow (Pierson, 2005). A soluble white precipitate commonly coated many clasts on the surface of the deposit.

The extent of the April 4 lahar was mapped on a satellite image obtained on the afternoon of April 4 (fig. 13). The color of the lahar deposit contrasted markedly with adjacent snow cover (fig. 12), which permitted easy recognition and detailed mapping of the deposit. The April 4 lahar inundated an area of about 125 km^2, an area up to 20 percent greater than that inundated by the March 23 lahar, whose total extent was partly obscured by snow. Field visits to the Drift River valley after April 4 allowed us to examine both lahar deposits and to document high-water marks of the April 4 lahar left primarily as mud lines on trees. Generally, it was possible to measure the height of mud lines above the nearest active channel to estimate maximum local flow depth and run up. These measurements are used below to estimate discharge and volume.

Comparison of Deposits

Samples of lahar matrix collected from both the March 23 (n=2) and April 4 (n=17) deposits were sieved to determine particle-size distributions of material smaller than 4 mm. The results of these analyses indicate that the April 4 deposit consists mainly of fine-skewed, poorly sorted, fine-to-coarse sand, whereas the two March 23 samples were slightly coarser and less well sorted (fig. 16). One

sample, collected from the distal northern margin of the April 4 deposit (sample R, fig. 17), consists of about 90 percent silt and finer material and probably records tranquil standing water conditions at this location. The April 4 deposit shows only minor variation and no apparent spatial trend in sand and silt content, sorting, and mean grain diameter (fig. 17). This suggests that the April 4 lahar underwent little to no flow transformation as it progressed downstream.

Discharge and Volume Estimates

Information about the hydraulic characteristics of the 2009 lahars was derived from field observations, analysis of satellite images, and indirect measurements of flow depth, run up, and width, and estimates of flow velocity. We have limited information about the flow characteristics of the March 23 lahar and thus provide only a generalized estimate of discharge for the upper part of the valley. The discharge and volume estimates for the April 4 event are better constrained but still approximate because of uncertainties associated with determining flow depth, width, and velocity. All discharge and volume estimates include substantial uncertainty.

Peak Discharge of March 23 Lahar

We were unable to document flow depths directly for any of the first three lahars of the eruption. Aerial photographs of the Dumbbell Hill area obtained after emplacement of the March 23 lahars indicate that the largest flow had a maximum width of about 2,000 m (figs. 6A, 7, 9B) and a maximum flow depth of 6–8 m; average flow depth probably was only 2–4 m. Cross-sectional areas inundated by the largest of these lahars probably were on the order of 4,000–8,000 m^2. Lahar run up observed on the upstream end of Dumbbell Hill was estimated in the field to be about 13 m above the channel floor, indicating an approximate flow velocity of 16 ms^{-1} (estimated from a flow run-up equation). Application of the run-up equation assumes steady, uniform flow, which was unlikely for these ice-laden lahars. Debris flow velocity estimates made with this equation may be too high by 30 percent or more (Iverson and others, 1994). Furthermore, the ice-choked character of the flow may have created ice-shove, jamming, and other impediments. Thus, we use a range of values from 5 to 15 ms^{-1} for flow velocity. This suggests a peak discharge near Dumbbell Hill in the range of 20,000–120,000 m^3s^{-1} (or 10^4–10^5 m^3s^{-1}).

Peak Discharge of April 4 Lahar

Flow depth, width, and velocity at the time of peak discharge for the April 4 lahar were estimated both from field evidence and from data on hyperconcentrated lahars in the literature. Flow depth was estimated by measuring the height of sandy mud coatings (mud lines) on trees above nearby deposit surfaces and above nearby active channel beds. These values provide a possible range of flow depths at the time of peak discharge, but because the bed aggraded during the flow and perhaps incised during waning flow, it is not possible to know where the bed was when the flow coated the trees. At some field locations flow depths estimated from the height of mud lines above April 4 lahar terraces ranged from 0.4 to 5 m, with one site showing a local depth of about 6 m (fig. 18B). Maximum flow depths estimated from the heights of mud lines above the valley floor ranged from 1.4 to 13 m (fig. 13). Maximum flow width normal to the flow path was scaled from satellite images, although in the lower reach it is unlikely that flow occupied all channels simultaneously. Flow velocities could not be indirectly estimated in the field for this lahar, so velocities of similar hyperconcentrated flows at similar flow depths on similar channel slopes were used to help constrain estimates (Pierson, 2005).

Channel cross sections (fig. 19) were derived from a 10-m DEM of the Drift River valley made from August 1990 topographic data acquired by the U.S. Geological Survey. The cross sections give approximate channel dimensions and are broadly representative of the channel shape at the time of the 2009 lahars, possibly to within several meters. We have no way to independently verify the pre-lahar channel geometry and were unable to obtain topographic data of the valley after the eruption ended. The initial wave of the April 4 lahar was flowing over a valley floor that had been inundated by 18 previous lahars, including the extensive lahars of March 23 and 26. The valley floor was covered with a fill of sand, gravel, and slabs of ice from these events and intervening streamflow; some of this material was frozen. The degree of dissection of the valley floor is not known, but observations made on March 26 indicated that flows subsequent to March 23 had eroded parts of the valley floor, particularly along the main channel of the Drift River.

In the lower part of the valley at cross-section 8, west of the DRMT (fig. 14), we assume that between one-half and all of the valley cross section was occupied by flow at the peak stage of the April 4 lahar. A satellite image and oblique aerial photographs (figs. 12B and 13) obtained on the afternoon of April 4 indicate that the entire cross section had been inundated. However, other studies have shown that the fronts of hyperconcentrated-flow lahars can be sediment depleted and erosive (Pierson, 2005), which could cause the head of the lahar (typically the flow peak or shortly behind) to incise the channel. If this happened when the April 4 lahar entered Rust Slough and passed by the DRMT, it is possible that the peak discharge of the lahar did not correspond with maximum inundation at the cross section, and thus our estimate of cross-sectional flow area would be too high. The height of mud lines above nearby active channel beds near cross-section 8 ranged from 1.5 to 4 m (fig. 13); the average flow depth is estimated at 2 m. High sediment-concentration water floods and hyperconcentrated-flow lahars can cause flow to rapidly shift laterally in a valley (for example, Scott and others, 1996), so the flow probably was dispersed among multiple braided channels with intervening bars and islands. As described in Dorava and Meyer (1994), average flow velocity of the January 2, 1990, lahar in the lower Drift River valley was perhaps as large as 4 ms^{-1}, and comparable hyperconcentrated flows at other volcanoes have had flow velocities of 2–4 ms^{-1} (Pierson, 2005). Thus, we use average flow velocities of 1 and 5 ms^{-1} to estimate possible discharges of the lahar in the lower part of the Drift River valley (table 3). We find that a reasonable range of peak discharges for a lahar occupying all of cross-section 8, with an average depth of 2 m, is 6,000–33,000 m^3s^{-1}. If only one-half of cross-section 8 (width = 1,600 m) was inundated at the peak stage of the lahar, the range of discharges would be 3,200–16,000 m^3s^{-1} (table 3). Thus, an order-of-magnitude estimate of peak discharge for the April 4 lahar at the DRMT is about 10^3–10^4 m^3s^{-1}.

Peak discharge in the upper reach of the Drift River is more difficult to estimate because the initial flood wave was flowing, at least in part, on the surface of the frozen March 23 lahar deposits (fig. 14A), which (1) filled a portion of the upper valley cross section to an unknown depth, (2) undoubtedly had an uneven surface topography, and (3) had been locally incised or buried by as many as 17 lahars between March 24 and March 30 (figs. 3, 9A, and 9B). Thus, it is impossible to know where the channel bed was or precisely what the flow depth was when the April 4 lahar passed through. However, an order-of-magnitude estimate can be posited for cross section 1, on the basis of known flow width (fig. 13), indirect measurements of the 1989–90 lahar velocities (3–23 ms^{-1}; Dorava and Meyer, 1994), and two indirect calculations of velocity along the main axis of April 4 flow, based on flow run-up on Dumbbell Hill and the adjacent north valley wall (16 and 23 ms^{-1}). The elevation of high-water marks measured in the area of cross-section 1 (fig. 13) averaged about 8 m above the valley floor, but we are not confident that this is a reasonable value for average flow depth. If the channel floor was aggrading during the peak stage of the flow, the average depth would have been less than this value, and if the channel was incising, it might have been locally greater. Thus, an average flow depth in the range of 2–5 m seems reasonable. Our best estimates of the hydraulic variables are a flow width of 2,100 m

(assuming all valley width was occupied), average depth of 2–5 m (thinner on margins, deeper along flow axis), and an average flow velocity of 10–15 ms^{-1}. These values give a range in peak discharge of 42,000–157,000 m^3s^{-1}, or 10^4–10^5 m^3s^{-1}, values that are roughly the same order of magnitude as those estimated for 1990 lahars (12,000–80,000 m^3s^{-1}; Dorava and Meyer, 1994). The discharge estimates for the 1990 lahars were made using slope-conveyance and slope-area techniques, both of which assume steady, uniform flow (Dorava and Meyer, 1994). Although these techniques generally are not applicable to lahars, they provide order of magnitude estimates of flow discharge.

Lahar Volume Estimates

Rough estimates of flow volumes were obtained for the March 23 and April 4 lahars in two ways: (1) by multiplying deposit area by estimated average deposit thickness; and (2) by converting ice-loss volumes to water equivalence, and then multiplying by a sediment (or ice) bulking factor to achieve the solids concentrations inferred from deposit sedimentology. Considerable error is inherent in both methods, given the available data and high degree of uncertainty in assumptions of such factors as cross-sectional areas of flows, average deposit thickness, and amount of ice loss that provided water to mobilize lahars. For the first method, inundation areas digitized from aerial photographs and satellite imagery are among the best-constrained factors, at least for lahars of March 23 and April 4. Estimates of deposit thickness are based on scattered observations throughout the valley, many of which come from marginal areas. For the second method, areas of ice loss were determined from satellite imagery and oblique aerial photographs and multiplied by estimates of ice thickness from 1989 to 1990 data (Trabant and Hawkins, 1997) to provide order-of-magnitude ice-loss volumes. Ice loss volumes were converted to water equivalents and multiplied by sediment bulking factors (Scott, 1988), which were inferred from deposit textures.

Within the uncertainties of the methods used for evaluation, estimates of the volumes of the largest lahars of the 2009 eruption range from 10^7 to 10^8 m^3 (table 4). The combined volume of the two large March 23 lahars is estimated to range from 2 to 20 $\times 10^7$ m^3, so the volume of each individual flow must have been on the order of 10^7–10^8 m^3. The March 26 lahar appears to have had a volume of about 10^7 m^3 estimated on the basis of an area-average deposit thickness calculation. The volume of the April 4 lahar is estimated to fall within the range of 6–25$\times 10^7$ m^3. The estimated peak discharges and volumes are consistent with published correlations of peak discharge to flow volume for debris-flow lahars and nonvolcanic debris flows (Mizuyama and others, 1992; Rickenmann, 1999; and Jakob, 2005). Thus, the two ice-slurry lahars on March 23 and the dominantly hyperconcentrated-flow lahar on April 4 all appear to have had volumes of the same order of magnitude as the largest lahar of the 1989–90 eruption on January 2, 1990 (Gardner and others, 1994), and probably of the same order of magnitude as other historic and prehistoric lahars caused by eruption of this volcano.

Discussion

The lahars produced early in the 2009 eruption on March 23 were strikingly different in composition and flow type compared to the similarly sized April 4 lahar emplaced at the end of the explosive phase of the eruption. The March 23 flows were highly mobile, water-saturated granular mass flows composed predominantly of ice fragments—ice-slurry lahars. Small ice-rich mass flows with varying water contents have been previously described having been triggered by (a) liquid water explosively ejected out of crater lakes onto snowfields (Cronin and others, 1996; Lube and others, 2009; Kilgour and others, 2010); and (b) loading of snow slopes with explosively ejected ballistics or pyroclastic flows (Waitt and others, 1983; 1994; Pierson and others, 1990; Pierson and Janda, 1994). The ice-slurry lahars emplaced on March 23 were at least several times larger and traveled tens of

kilometers farther than previously described ice-rich mass flows. A key factor in the development of the ice-rich lahars on March 23 was the availability of snow and ice—Drift glacier at full volume and extensive, thick snowpack and river ice (as much as 2 m) in the Drift River valley. Outcrops of the March 23 ice-rich lahar showed no apparent systematic downstream changes in internal structure. In contrast, the April 4 lahar contained small amounts of ice relative to the March 23 lahars; some of this ice was eroded from the Drift glacier and some of it was reworked from the March 23 deposits. The April 4 flow probably began as a debris-flow lahar but quickly transformed to a more dilute hyperconcentrated-flow lahar as it progressed down the Drift River valley.

Recent historical eruptions of Redoubt Volcano have all been characterized by vent-clearing explosive activity followed by episodic dome growth and destruction (Miller, 1994), which led to extensive lahars and flooding in the Drift River valley (Sturm and others, 1986; Dorava and Meyer, 1994). Failures of large lava domes that grew in the summit crater have produced pyroclastic flows and voluminous lahars. Failure of the largest lava domes of the 1989–90 eruption produced large lahars on January 2 (dome volume about 3×10^7 m^3) and February 15, 1990 (dome volume about 1.5×10^7 m^3) (Dorava and Meyer, 1994; Miller, 1994). Explosive event 19 on April 4, 2009, also was accompanied by a dome failure, which led to the largest lahar of the 2009 eruption. Although the exact volume of the dome that failed on April 4 is not known, estimates range up to 3.6×10^7 m^3 similar to the volume of the lava dome that failed on January 2, 1990. On the basis of approximate volumes of failed domes and estimated volumes of lahars, it appears that eruptions of Redoubt Volcano involving failures of lava domes having volumes of about 10^7 m^3 tend to produce lahars having volumes in the range of 10^7–10^8 m^3.

Although it is clear that swift melting of glacier ice by pyroclastic flows created by dome collapse led to formation of the large lahar on April 4, 2009, the mechanism of water generation associated with the March 23, 2009, lahar is less obvious. Because the lahars emplaced on March 23 were composed almost entirely of ice fragments, and none of the rare volcanic rock fragments examined in the field were obviously juvenile, evidence for pyroclastic flow involvement in meltwater generation is weak. However, proximal tephra deposits associated with explosive event 5 contained angular, pebble-sized ice clasts as well as dense to vesicular juvenile fragments (majority) and non-juvenile lithic clasts (Schaefer, 2012), indicating that ice, pre-existing rock, and juvenile magma were explosively fragmented and ejected from the ice-filled summit crater. It is possible that explosive activity in the summit crater generated some meltwater by thermal and mechanical interaction with snow and ice around the vent. It also is possible that some water was ejected along with ice fragments from the crater. Such water may have accumulated beneath or within the summit crater ice as a result of fumarolic heating, and some may have come from water-saturated rock around the vent. It also is possible that a small dome may have grown in the vent during the nearly 3-hour interval between explosive events 4 and 5. If so, and if it grew at the maximum estimated extrusion rate of 2009 (35 m^3s^{-1}, Diefenbach and others, 2012), then a modest-sized lava dome of about $3–4\times10^5$ m^3 could have been present. If such a dome had failed and rapidly fragmented, then a pyroclastic flow traveling a short distance over the upper Drift glacier could have produced some meltwater. The eruption columns generated during explosive events 4 and 5 lofted to about 14–18 km above sea level and were among the largest of the eruption sequence. A limited run-out pyroclastic flow possibly could have formed locally around the base of the eruption column and been funneled down the upper Drift glacier resulting in melting that led to the March 23 lahar. However, no pyroclastic-flow deposits were observed in the field, and it is unlikely that they would have been easily differentiated from thick tephra deposits high on the flanks of the volcano. Substantial ice was lost from the Drift glacier between March 20–26, and ice was most likely lost during the explosive events that triggered the lahars of March 23.

Large flows composed of ice and water often result from the release of ice jams that occur during the breakup of winter ice cover in rivers (Beltaos, 2008). Water stored behind an ice jam can be released suddenly and produce significant flood waves or surges consisting of fragmented, highly concentrated masses of ice and water known as "ice runs" (Jasek, 2003). Ice runs may be unimpeded if they encounter open water downstream, or be impeded if they encounter intact ice cover downstream. A sudden release of water by the eruptive events of March 23 is possibly analogous to the release of an ice jam, and the subsequent formation of the ice-rich lahar analogous to an impeded ice run. Impeded ice runs progress downstream as moving masses of ice rubble, and they can push through and incorporate intact ice or stop and create a new ice jam. The March 23 lahar possibly developed as meltwater and rafted glacier ice encountered the frozen, snow-covered floor of the Drift River valley and formed a temporary ice jam. If such a jam or jams formed and failed, the flow may have behaved as an ice run and formed the ice-rich deposit we observed, which looked similar to the chaotic assemblages of river ice associated with severe ice jam floods (Beltaos, 2008).

Dome-building eruptions that produce pyroclastic flows when the Drift glacier is near or at its full modern volume of about 1 km^3 can produce sufficient external water to generate large lahars in the Drift River valley. The pyroclastic flows need not be especially large to produce meltwater because glacier ice and snow are readily available in the upper Drift River valley. Throughout the course of historical eruptions at Redoubt, ice has been repeatedly removed from the gorge of the upper Drift glacier above an altitude of about 700 m by pyroclastic flows and dome-collapse debris (Trabant and others, 1994). When ice in the gorge is gone, the only significant source of meltwater for large lahars is the piedmont lobe of the glacier, an area of the valley that is wide, has a low surface slope, and is not topographically restricted. Pyroclastic flows that reach the piedmont lobe spread laterally and are much less spatially concentrated unless funneled into ice canyons. Thus, after ice is removed from the gorge area, considerably larger, longer run-out pyroclastic flows may be required to erode ice from the piedmont lobe to produce meltwater for lahars. However, much of the piedmont lobe has a cover of supraglacial debris that could restrict thermal and mechanical erosion by pyroclastic flows. Thus, as eruptions progress, potential water sources may diminish and lessen the ability of an eruption to generate lahars (Trabant and others, 1994).

The volumes and peak discharges of the 2009 lahars were of the same order of magnitude as the 1989–90 lahars, and probably also the 1966 lahars. The largest lahars had volumes of about 10^7–10^8 m^3 and achieved peak discharges up to 10^4–10^5 m^3s^{-1}. The total number of smaller lahars triggered also was roughly similar for the two eruptions—at least 18 in 1989–90 (Brantley, 1990) and 20 in 2009.

Significantly larger lahars than those witnessed historically could be generated by events of a scale more rare in Redoubt's past. Voluminous lahars associated with debris avalanches could be generated by sector collapses of part of the Redoubt volcanic edifice, and some evidence exists that this has happened possibly several times in the past 10,000 years (Riehle and others, 1981; Begét and Nye, 1994). Lahars larger than those of the past three historical eruptions also might accompany a more voluminous and longer duration explosive eruption. Pyroclastic flows sweeping a broader area of snow and ice in the Drift River basin could generate significantly larger meltwater and lahar volumes (Waythomas and others, 1997).

The degree of hazard in the lower Drift River valley is not simply a function of lahar magnitude, however. A series of smaller lahars and floods can incrementally aggrade the valley floor by transporting and depositing massive volumes of sediment. Such aggradation can clog the existing channels and allow subsequent smaller flows to reach higher levels. Furthermore, aggradation can lead to lateral shifting of the river. High-discharge dilute flows that can occur late in an eruptive cycle can cause vertical or lateral erosion in the lower valley, which also can result in significant channel avulsion. Lateral shifting can allow flows to more directly impinge on protective structures at DRMT, and incision can cause scour of channels that cross the buried pipeline, as occurred in 1990 (Dorava and Meyer, 1994).

Huge quantities of sediment were mobilized by lahars in the Drift River valley during the 2009 eruption and triggered rapid changes. By summer 2010, as much as 10 m of incision through the 2009 lahar deposits (and possibly the underlying alluvium) had occurred in the upper Drift River valley. This channel incision contributed additional sediment downstream, which caused the main channel of the lower Drift River and the Rust Slough–Cannery Creek drainage (fig. 7) to aggrade by several meters. As the Drift River erodes and redistributes, the volcaniclastic sediment, downstream aggradation, and possibly river avulsion, is likely to continue for many years, which may induce greater than usual river stages and flooding along the lower Drift River and its distributary channels.

Eruption-induced lahars in the Drift River valley are much larger than the flows that can be produced by rainfall runoff. Documented flood peaks in drainages throughout south-central Alaska (Jones and Fahl, 1994) provide a general estimate for the largest meteorologically generated flows possible in the region (fig. 20) and indicate a maximum water flood peak discharge of about 2,000 m^3s^{-1} for the Drift River (drainage area = 570 km^2). Using regional flood-frequency equations described in Curran and others (2003), the estimated 100-year and 500-year-flood peak discharges for the Drift River drainage are about 1,000 and 1,300 m^3s^{-1}, which are tens to hundreds of times smaller than historical Redoubt lahars. The estimated peak discharge of the April 4 lahar near the DRMT (fig. 13, cross-section 8), which is more directly comparable to the regional flood-frequency estimate of the 100-year flood peak, was 3,000–33,000 m^3s^{-1} and at least 3–30 times larger than the estimated 100-year flood peak. Clearly, eruption-generated flow discharges can be much larger than those generated by rainfall or normal snowmelt.

Conclusions

Redoubt Volcano regularly produces large (discharges to 10^4 m^3s^{-1} and volumes to 10^6 m^3) to very large (discharges to 10^5 m^3s^{-1} and volumes to 10^8 m^3) lahars of varying character during eruptions—most recently in 2009 but also documented in 1989–90 and 1966. These lahars are primarily triggered by the rapid melting of snow and ice on the north-flank Drift glacier by explosive events and pyroclastic flows resulting from collapses of growing lava domes. This volcano is so effective at producing voluminous lahars in part because the topography of its upper northern flank concentrates pyroclastic flows into a narrow, steep bedrock gorge that is occupied by the upper part of the glacier. This allows large volumes of snow and ice to be entrained and melted rapidly. As witnessed during the past few decades, much of this lost volume can be replaced in a few decades or less.

The primary conclusions of our analysis of lahar generation during the 2009 eruption are:

- Explosive activity from March 23 to April 4 produced lahars having volumes of 10^7–10^8 m^3 and peak discharges of 10^4–10^5 m^3s^{-1}—flows almost two orders of magnitude larger than can be generated by rainstorms or seasonal snowmelt in this region and comparable in size to the largest lahars generated in 1989–90 and probably also in 1966. Even larger lahars could be generated by structural failure of the volcanic edifice (sector collapse), or by pyroclastic flows larger than those documented during the 1989–90 and 2009 eruptions.

- Two very large flows at the beginning of the explosive phase of the eruption, only hours apart on March 23, were water-saturated granular mass flows composed almost entirely of ice fragments and water—ice-slurry lahars—that flowed down the 35-km-length of the Drift River valley beyond Drift glacier to Cook Inlet. Volcanically generated ice-slurry lahars of this magnitude are unusual and apparently unprecedented in the literature.
- The very large lahar generated on April 4 at the end of the sequence of explosive activity had a very different composition and character from the earlier ice-slurry lahars. This lahar contained relatively little ice, and rather than being a granular, debris-flow lahar, it was a more dilute hyperconcentrated-flow lahar.
- In addition to these large to very large lahars, at least 17 additional smaller lahars and floods were generated in late March.

Redoubt Volcano has erupted more than 50 times in the past 10,000 years and 4 times since 1900. During the three eruptions of the past 46 years, each has produced numerous lahars in the Drift River valley. Another eruption and hazardous lahars down the Drift River during next 20–30 years would not be unusual or unexpected.

In addition to their direct impacts, lahars can have secondary impacts on valley morphology and fluvial processes. Incision of lahar deposits in the upper and middle parts of the Drift River valley has supplied sediment leading to distal channel aggradation, and bed elevations in the lower Drift River valley have risen by several meters. Continued aggradation of the lower Drift River will maintain elevated channel beds and promote overbank flooding during periods of high runoff, or should eruptive activity resume, during even small- to moderate-sized lahars.

Acknowledgments

The authors thank the staff of Lake Clark National Park and Preserve for facilitation of our work within the park. We appreciate and gratefully acknowledge the support of the staff and operators of the Drift River Marine Terminal. Manuscript reviews provided by Dave Meyer and Game McGimsey (both U.S. Geological Survey) and discussions with Kate Bull (Alaska Division of Geological and Geophysical Surveys), Kristi Wallace (U.S. Geological Survey), Chris Nye (Alaska Division of Geological and Geophysical Surveys), and Bob Swenson (Alaska Division of Geological and Geophysical Surveys) helped clarify several aspects of the work.

References Cited

Begét, J.E., and Nye, C.J., 1994, Postglacial eruption history of Redoubt Volcano, Alaska, *in* Miller, T.P., and Chouet, B.A., eds., The 1989–1990 eruptions of Redoubt Volcano, Alaska: Journal of Volcanology and Geothermal Research, v. 62, p. 31–54.

Beltaos, S., 2008, River Ice Breakup: Highlands Ranch, Colo., Water Resources Publications, 480 p.

Brantley, S.R. (ed.), 1990, The eruption of Redoubt Volcano, Alaska, December 14, 1989–August 31, 1990: U.S. Geological Survey Circular 1061, 33 p.

Coombs, M.L., Sisson, T.W., Bleick, H.A., Henton, S.M., Nye, C.J., Payne, A.L., Cameron, C.E., Larsen, J.F., Wallace, K.L., and Bull, K.F., 2012, Andesites of the 2009 eruption of Redoubt Volcano, Alaska: Journal of Volcanology and Geothermal Research, doi: 10.1016/j.jvolgeores.2012.01.002.

Cronin, S.J., Neall, V.E., Lecointre, J.A., and Palmer, A.S., 1996, Unusual "snow slurry" lahars from Ruapehu volcano, New Zealand, September 1995: Geology, v. 24, p. 1107–1110.

Curran, J.H., Meyer, D.F., and Tasker, G.D., 2003, Estimating the magnitude and frequency of peak streamflows for ungaged sites on streams in Alaska and conterminous basins in Canada: U.S. Geological Survey Water-Resources Investigations Report 03–4188, 101 p.

Diefenbach, A.K., Bull, K.F., Wessels, R.L., and McGimsey, R.G., 2012, Photogrammetric monitoring of lava dome growth during the 2009 eruption of Redoubt Volcano: Journal of Volcanology and Geothermal Research, doi:10.1016/j.jvolgeores.2011.12.009.

Dorava, J.M., and Meyer, D.F., 1994, Hydrologic hazards in the lower Drift River basin associated with the 1989–90 eruptions of Redoubt Volcano, Alaska: Journal of Volcanology and Geothermal Research, v. 62, p. 387–407.

Gardner, C.A., Neal, C.A., Waitt, R.B., and Janda, R.J., 1994, Proximal pyroclastic deposits from the 1989–1990 eruption of Redoubt Volcano, Alaska, *in* Miller, T.P., and Chouet, B.A., eds., The 19891990 eruptions of Redoubt Volcano, Alaska: Journal of Volcanology and Geothermal Research, v. 62, p. 213–250.

Iverson, R.M., LaHusen, R.G., Major, J.J., and Zimmerman, C.L., 1994, Debris flow against obstacles and bends; dynamics and deposit: Eos, Transactions, American Geophysical Union Fall Meeting Abstracts, v. 75, no. 4, p. 274.

Jakob, M., 2005, A size classification for debris flows: Engineering Geology, v. 79, p. 151–161.

Jasek, M., 2003, Ice jam release surges, ice runs, and breaking fronts; field measurements, physical descriptions, and research needs: Canadian Journal of Civil Engineering, v. 30, p. 113–127.

Jones, S.H., and Fahl, C.B., 1994, Magnitude and frequency of floods in Alaska and conterminous basins of Canada: U.S. Geological Survey Water-Resources Investigations Report 93-4179, 122 p.

Kilgour, G., Manville, V., Pasqua, F.D., Graettinger, A., Hodgson, K.A., and Jolly, G.E., 2010, The 25 September eruption of Mount Ruapehu, New Zealand; directed ballistics, surtseyan jets, and ice-slurry lahars: Journal of Volcanology and Geothermal Research, v. 191, p. 1–14, doi:10.1016/j.jgeovolres.2009.10.015.

Lube, G., Cronin, S.J., and Procter, J.N., 2009, Explaining the extreme mobility of volcanic ice-slurry flows, Ruapehu volcano, New Zealand: Geology, v. 37, p. 15–18.

Major, J.J., and Newhall, C.G., 1989, Snow and ice perturbation during historical volcanic eruptions and the formation of lahars and floods: Bulletin of Volcanology, v. 52, p. 1–27.

Major, J.J., Pierson, T.C., and Scott, K.M., 2005, Debris flows at Mount St. Helens, Washington, USA, *in* Jakob, M., and Hungr, O., eds., Debris-flow Hazards and Related Phenomena: Chichester, UK, Springer-Praxis, p. 685-731.

Miller, T.P., 1994, Dome growth and destruction during the 1989–1990 eruption of Redoubt Volcano, *in* Miller, T.P., and Chouet, B.A., eds., The 1989–1990 eruptions of Redoubt Volcano, Alaska: Journal of Volcanology and Geophysical Research, v. 62, p. 197–212.

Mizuyama, T., Kobashi, S., and Ou, G., 1992, Prediction of debris flow peak discharge: Proceedings, International Symposium Interpraevent 4, p. 99–108.

Mothes, P.A., Hall, M.L., and Janda, R.J., 1998, The enormous Chillos Valley lahar; an ash-flow-generated debris flow from Cotopaxi Volcano, Ecuador: Bulletin of Volcanology, v. 59, p. 233–244.

Pierson, T.C., 1998, An empirical method for estimating the travel times for wet volcanic mass flows: Bulletin of Volcanology, v. 60, p. 98–109.

Pierson, T.C., 2005, Hyperconcentrated flow—transitional process between water flow and debris flow, *in* Jakob, M., and Hungr, O., eds., Debris-flow Hazards and Related Phenomena: Berlin, Springer, p. 159–202.

Pierson, T.C., and Janda, R.J., 1994, Volcanic mixed avalanches; a distinct eruption-triggered mass-flow process at snow-clad volcanoes: Geological Society of America Bulletin, v. 106, p. 1351–1358.

Pierson, T.C., Janda, R.J., Thouret, J-C., and Borrero, C.A., 1990, Perturbation and melting of snow and ice by the 13 November 1985 eruption of Nevado del Ruiz, Colombia, and consequent mobilization, flow and deposition of lahars: Journal of Volcanology and Geothermal Research, v. 41, p. 17–66.

Rickenmann, D., 1999, Empirical relationships for debris flows: Natural Hazards, v. 19, p. 47–77.
Riehle, J.R., Kienle, J., and Emmel, K.S., 1981, Lahars in Crescent River Valley, Lower Cook Inlet, Alaska: Alaska Division of Geological and Geophysical Surveys Geologic Report 53, 10 p.
Schaefer, J.G., ed., 2012, The 2009 eruption of Redoubt Volcano, Alaska: Alaska Division of Geological and Geophysical Surveys Report of Investigation 2011-5, 45 p.
Schiff, C.J., Kaufman, D.S., Wallace, K.L., and Ketterer, M.E., 2010, An improved tephrochronology of Redoubt Volcano, Alaska: Journal of Volcanology and Geothermal Research, v. 193, p. 203–214.
Scott, K.M., 1988, Origins, behavior, and sedimentology of lahars and lahar-runout flows in the Toutle-Cowlitz River system: U.S. Geological Survey Professional Paper 1447-A, 74 p.
Scott, K.M., Janda, R.J., de la Cruz, E.G., Gabinete, E., Eto, I., Isada, M., Sexton, M., Hadley, K.C., 1996, Channel and sedimentation responses to large volumes of 1991 volcanic deposits on the east flank of Mount Pinatubo, *in* Newhall, C.G., Punongbayan, R.S., eds., Fire and Mud; Eruptions and Lahars of Mount Pinatubo, Philippines: Quezon City, Philippine Institute of Volcanology and Seismology and Seattle, University of Washington Press, p. 971-988.
Sturm, M., Benson, C., and MacKeith, P., 1986, Effects of the 1966–68 eruptions of Mount Redoubt on the flow of Drift Glacier, Alaska, U.S.A: Journal of Glaciology, v. 32, p. 355–361.
Till, A.B., Yount, M.E., and Bevier, M.L., 1994, The geologic history of Redoubt Volcano, Alaska, *in* Miller, T.P., and Chouet, B.A., eds., The 1989–1990 eruptions of Redoubt Volcano, Alaska: Journal of Volcanology and Geothermal Research, v. 62, p. 11–30.
Trabant, D.C., Waitt, R.B., and Major, J.J., 1994, Disruption of Drift glacier and origin of floods during the 1989–1990 eruptions of Redoubt Volcano, Alaska, *in* Miller, T.P., and Chouet, B.A., eds., The 1989–1990 eruptions of Redoubt Volcano, Alaska: Journal of Volcanology and Geothermal Research, v. 62, p. 369–385.
Trabant, D., and Hawkins, D.B., 1997, Glacier ice-volume modeling and glacier volumes on Redoubt Volcano, Alaska: U.S. Geological Survey Water-Resources Investigations Report 97–4187, 29 p.
Vallance, J.W., 2000, Lahars, *in* Sigurdsson, H., Houghton, B.F., McNutt, S.R., Rymer, H., and Stix, J. eds., Encyclopedia of Volcanoes: San Diego, Academic Press, p. 601–616.
Waitt, R.B., Gardner, C.A., Pierson, T.C., Major, J.J., and Neal, C.A., 1994, Unusual ice diamicts emplaced during the December 15, 1989, eruption of Redoubt Volcano, Alaska: Journal of Volcanology and Geothermal Research, v. 62, p. 409–428.
Waitt, R.B., Pierson, T.C., MacLeod, N.S., Janda, R.J., Voight, B., and Holcomb, R.T., 1983, Eruption-triggered avalanche, flood, and lahar at Mount St. Helens—effects of winter snowpack: Science, v. 221, p. 1394–1396.
Walder, J.S., 2000a, Pyroclast/snow interactions and thermally driven slurry formation. Part 1; theory for monodisperse grain beds: Bulletin of Volcanology, v. 62, p. 105–118.
Walder, J.S., 2000b, Pyroclast/snow interactions and thermally driven slurry formation. Part 2; experiments and theoretical extension to polydisperse tephra: Bulletin of Volcanology, v. 62, p. 119–129.
Waythomas, C.F., Dorava, J.M., Miller, T.P., Neal, C.A., and McGimsey, R.G., 1997, Preliminary volcano-hazard assessment for Redoubt Volcano, Alaska: U.S. Geological Survey Open-File Report 97–857, 40 p.

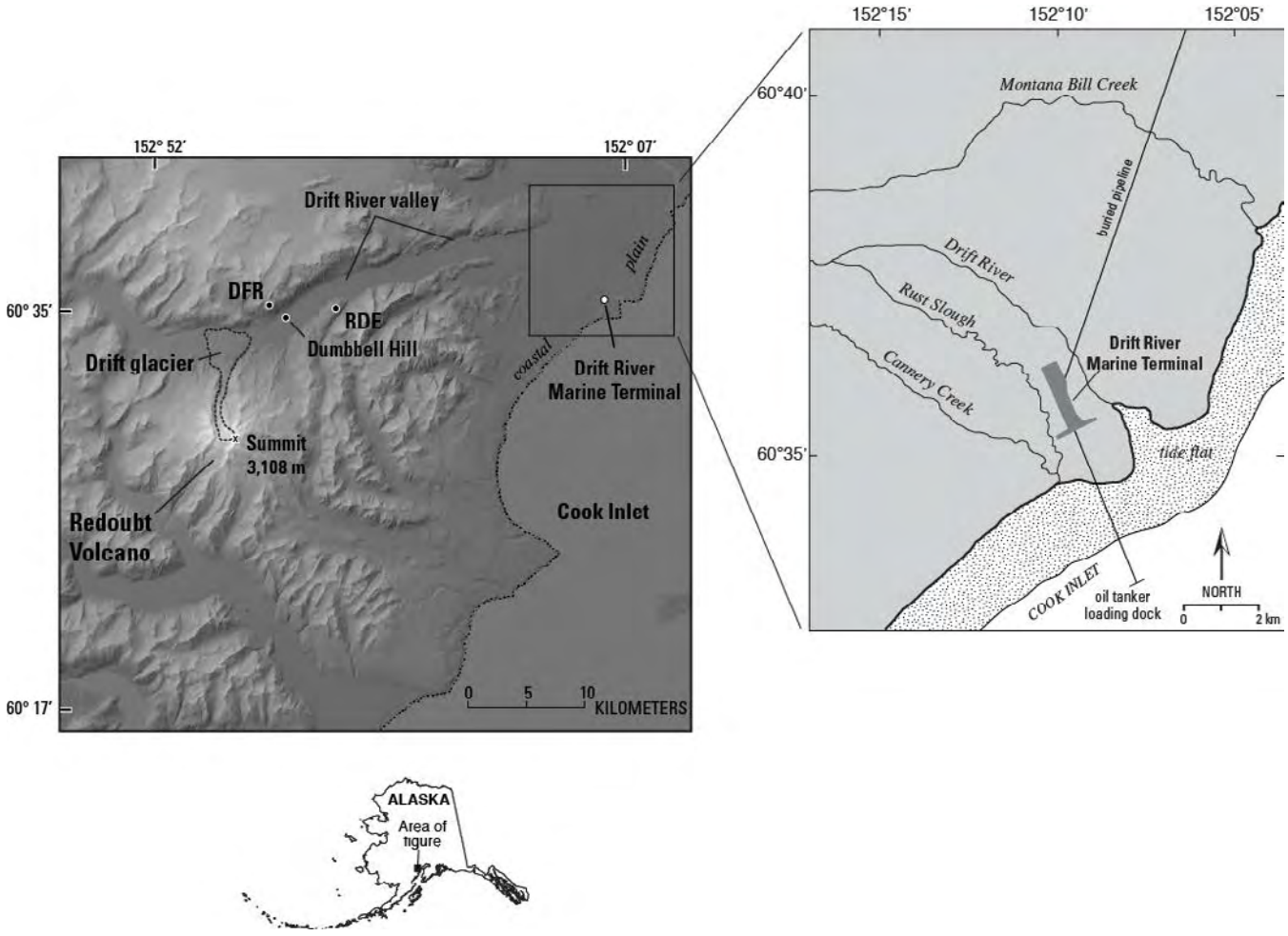

Figure 1. Shaded relief map of Redoubt Volcano and the Drift River valley, Alaska. The location of the Drift River Marine Terminal and seismic stations DFR and RDE also are shown. Inset map on right shows location of Montana Bill Creek, Rust Slough, Cannery Creek, and main channel of the lower Drift River.

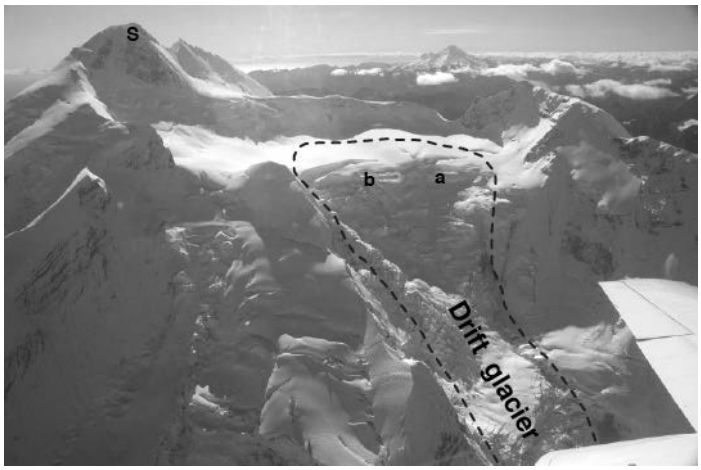

Figure 2. Photograph of summit crater of Redoubt Volcano, September 16, 2007. The dashed line indicates the approximate area of ice loss resulting from the 2009 eruption. The total amount of ice removed by the eruption was about 1–2.5×10^8 m^3. Letter **a** locates the last dome emplaced during the 1966–68 eruption, and letter **b** locates the last dome emplaced during the 1989–90 eruption. Feature labeled **S** is the summit (3,108 m). View is toward the southwest with Iliamna Volcano in background. Photograph by R.G. McGimsey, U.S. Geological Survey, Alaska Volcano Observatory.

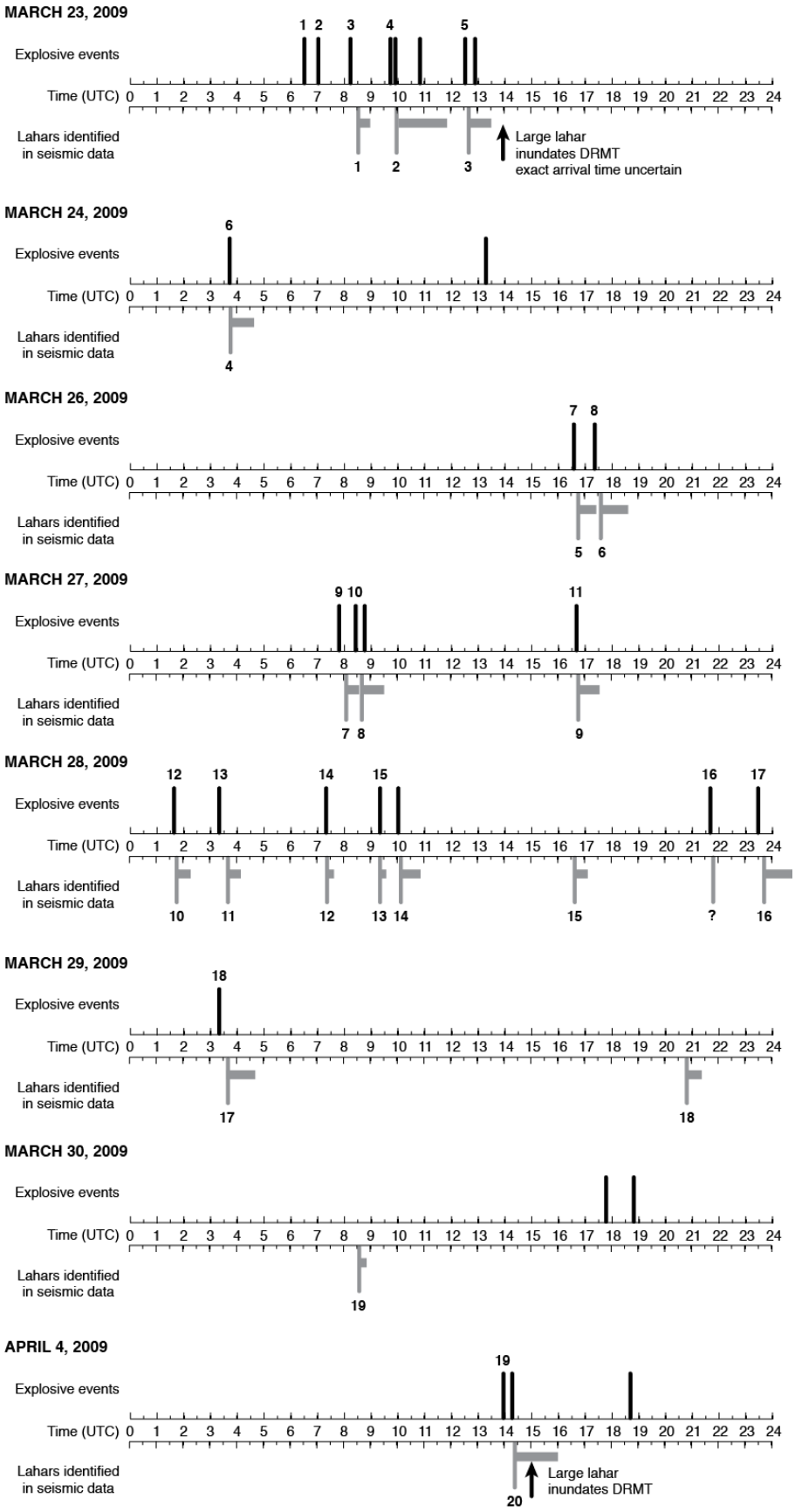
MARCH 23, 2009
Explosive events
Time (UTC)
Lahars identified in seismic data
Large lahar inundates DRMT exact arrival time uncertain
MARCH 24, 2009
MARCH 26, 2009
MARCH 27, 2009
MARCH 28, 2009
MARCH 29, 2009
MARCH 30, 2009
APRIL 4, 2009

Figure 3. Timeline of explosive events and lahars during the 2009 eruption. Black vertical bars indicate the time of the main numbered explosive events of the eruption and the unnumbered black vertical bars indicate the minor explosive events identified during reanalysis of seismic data (Schaefer, 2012). The gray vertical bars indicate the approximate time that lahar signals are detected in seismic data at stations DFR and RDE and are numbered consecutively to indicate individual lahars. The gray horizontal bars associated with the numbered lahars indicate the average duration of seismic signal at stations DFRand RDE where the signal is at least twice the background level. Locations of stations are shown in figure 1.

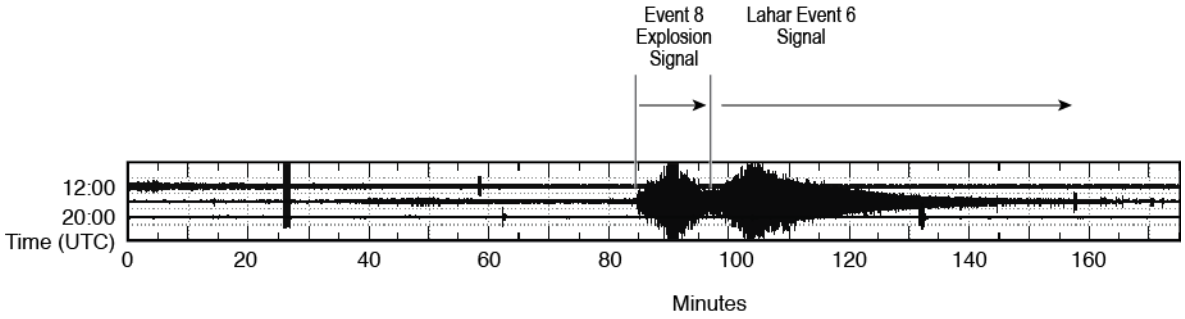

Figure 4. Helicorder record from seismic station RDE showing explosion and lahar signal associated with explosive event 8 and lahar event 6 on March 26, 2009. The character of the lahar signal shown here was typical of the lahar signals detected at stations DFR and RDE throughout the eruption.

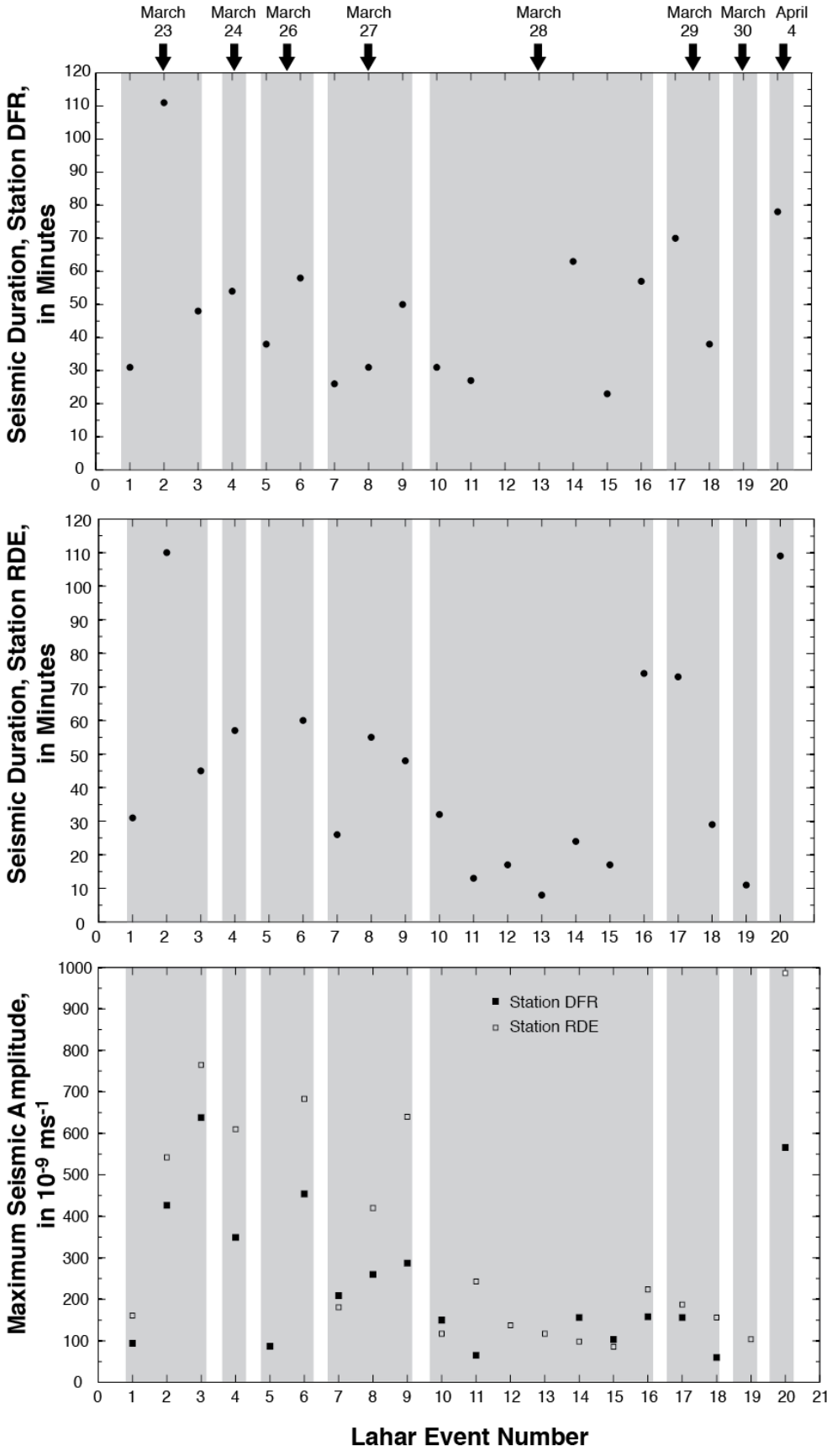
March 23
March 24
March 26
March 27
March 28
March 29
March 30
April 4
Seismic Duration, Station DFR, in Minutes
Seismic Duration, Station RDE, in Minutes
Maximum Seismic Amplitude, in 10-9 ms-1
Station DFR
Station RDE
Lahar Event Number

Figure 5. Seismic duration and maximum seismic amplitude at stations DFR and RDE for lahar events of the 2009 eruption. The differences in seismic duration among stations primarily are a result of variable path effects and the degree of coupling between the flow and the bed. Shaded area indicates time period of 1 day. Locations of stations are shown in figure 1.

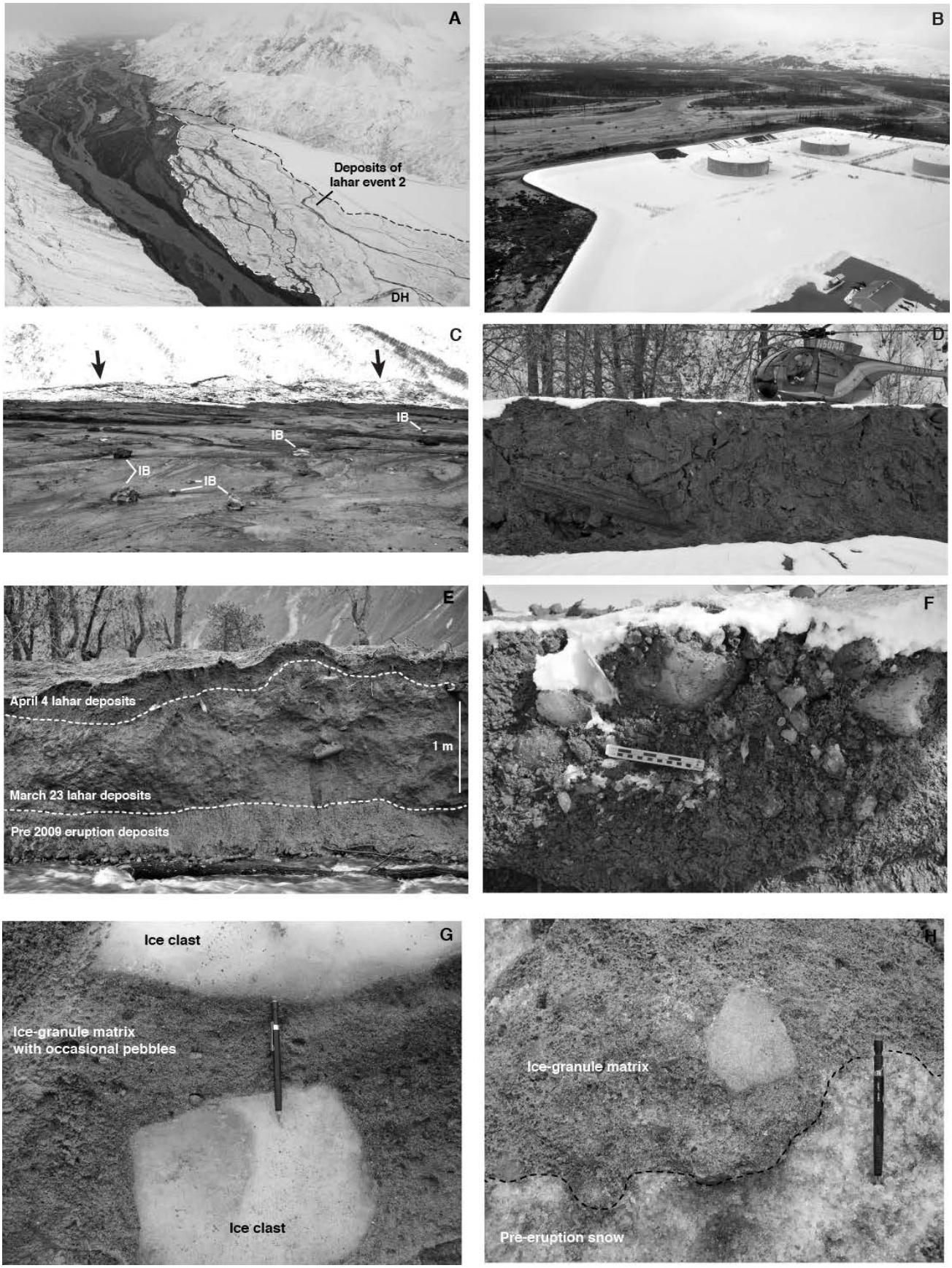
A
Deposits of
lahar event 2
DH
B
C
IB
IB
IB
IB
D
E
April 4 lahar deposits
1 m
March 23 lahar deposits
Pre 2009 eruption deposits
F
G
Ice clast
Ice-granule matrix
with occasional pebbles
Ice clast
H
Ice-granule matrix
Pre-eruption snow

Figure 6. Photographs of March 23 lahar deposits. A. View downstream (east) from station DFR. Inundation limits from two flows are evident. The snow-covered deposit probably was emplaced during lahar 2, whereas the area free of snow is likely the deposit from lahar event 3. Lahar event 3 occurred about 2.5 hours after lahar event 2, and minor snowfall occurred prior to lahar event 3. Photograph by R.G. McGimsey, U.S. Geological Survey, Alaska Volcano Observatory, March 23, 2009. B. Southwestern end of DRMT tank farm and protection levees showing minor lahar deposits on levee crest. Area of active flow is the Rust Slough–Cannery Creek drainage; flow direction is from right to left. Photograph by C. Read, U.S. Geological Survey, Alaska Volcano Observatory, March 23, 2009. C. View of the northern side of the Drift River channel showing maximum inundation limit of lahar 2 (arrows) and stranded ice blocks within deposits of lahar 3. The labeled ice blocks (IB) are 5–7 m in length; flow direction from left to right. Photograph by C. Read, U.S. Geological Survey, Alaska Volcano Observatory, March 23, 2009. D. Ice-rich lahar deposits consisting of imbricate tabular slabs of river and glacier ice exposed in cut bank along the Drift River. Photograph by C.F. Waythomas, U.S. Geological Survey, Alaska Volcano Observatory, April 17, 2009. E. Lahar deposits of 2009 eruption exposed along tributary to the Drift River south of Dumbbell Hill. Here, the March 23 deposits consist of an assemblage of subrounded to angular cobble to boulder-sized clasts of ice, logs and other vegetation, in a matrix of crushed ice and frozen meltwater. Photograph by C.F. Waythomas, U.S. Geological Survey, Alaska Volcano Observatory, May 22, 2009. F. Ice-rich lahar deposits exposed along Rust Slough at the DRMT. These deposits consist of rounded to subangular, cobble to small boulder sized clasts of ice in a fine-grained granular ice matrix. Length of scale is 15 cm. Photograph by C.F. Waythomas, U.S. Geological Survey, Alaska Volcano Observatory, March 26, 2009. G. March 23 lahar deposit matrix and rounded clasts of glacier ice. Matrix material consists of rounded granules of ice and occasional lithic pebbles. Photograph by T.C. Pierson, U.S. Geological Survey, Cascades Volcano Observatory, May 22, 2009. H. March 23 lahar deposit matrix and basal contact with underlying snow in the Drift River valley. Convoluted contact indicates incorporation of snow within lahar. Photograph by T.C. Pierson, U.S. Geological Survey, Cascades Volcano Observatory, May 22, 2009.

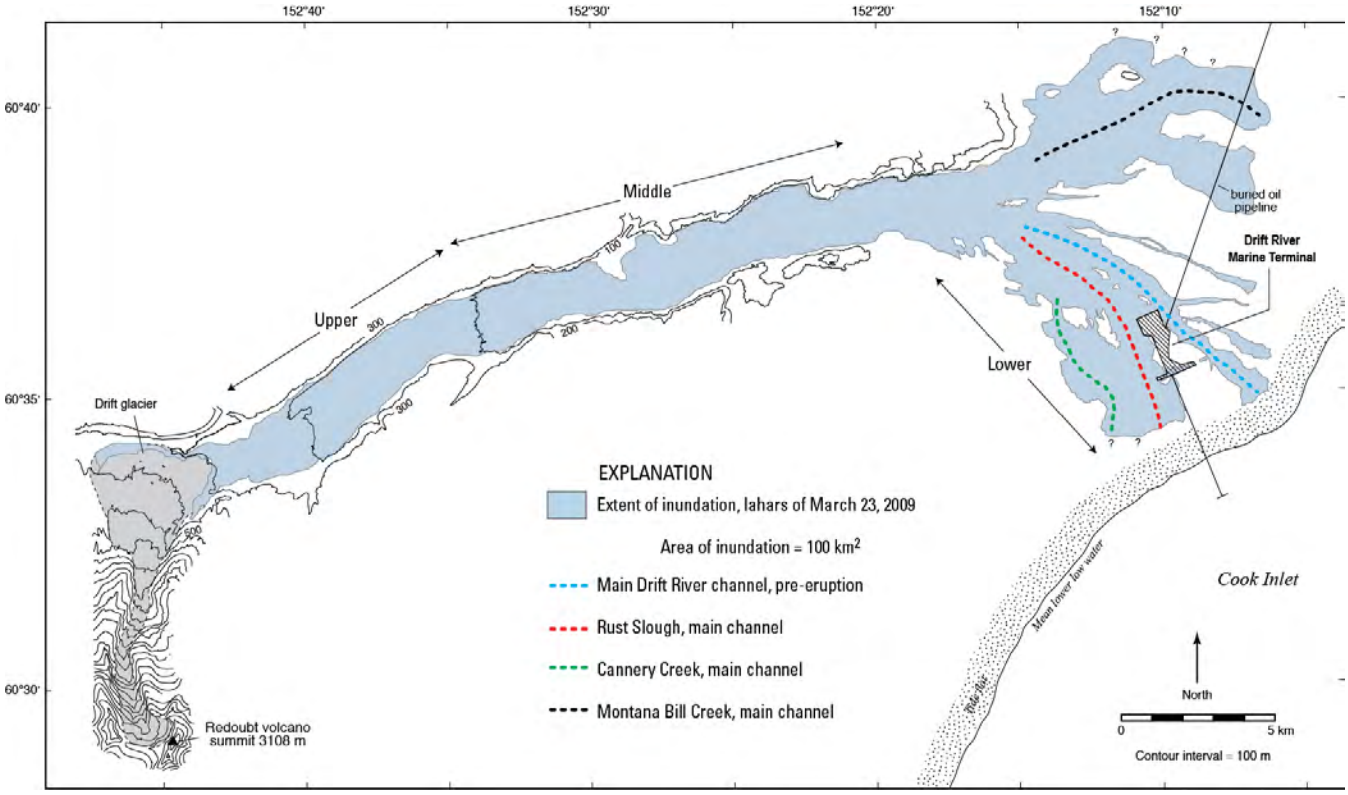

Figure 7. Map of March 23, 2009 lahar deposit in the Drift River valley. Extent deposit mapped on composite aerial photograph obtained by Aerometric, Inc., March 31, 2009. Snow cover obscured parts of the deposit, so extent queried where uncertain.

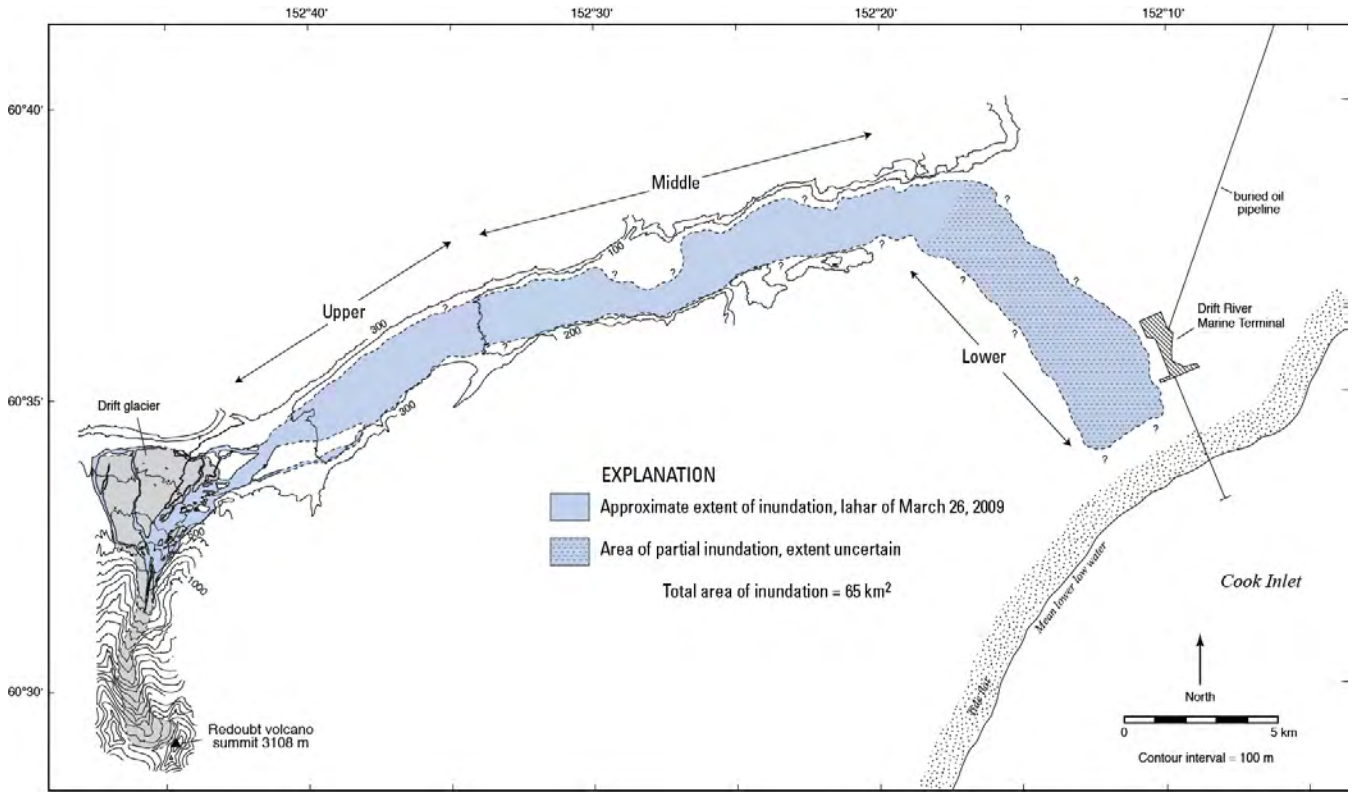

Figure 8. Map of March 26, 2009 lahar deposit in the Drift River valley. Extent of deposit determined from satellite image of the upper Drift River valley and oblique aerial photographs acquired on March 26, 2009. Extent of deposit in the lower Drift River drainage uncertain.

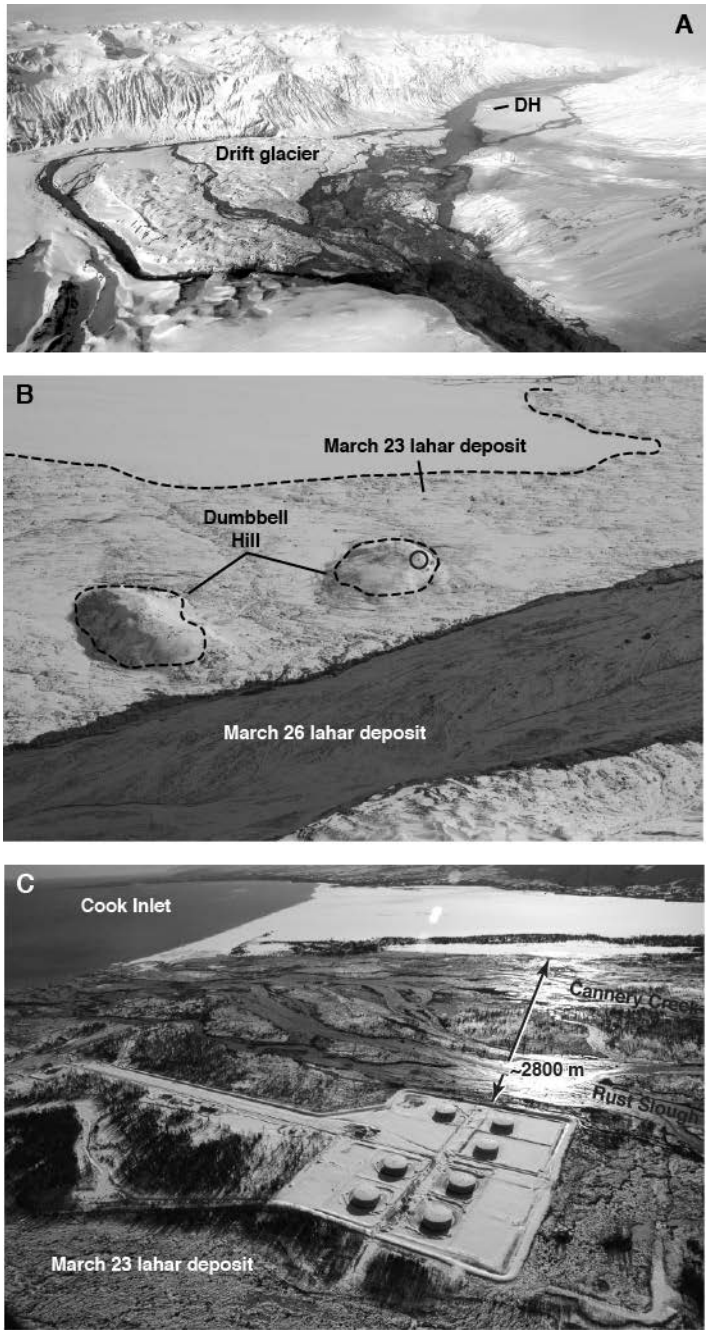

Figure 9. Photographs of March 26 lahar deposits taken during reconnaissance flight, afternoon of March 26, 2009. A. Upper Drift River valley and piedmont lobe of Drift glacier showing extent of inundation associated with lahars 5 and 6. DH shows location of Dumbbell Hill. B. Dumbbell Hill area showing extent of lahars of March 23 and 26. Circle on upstream (west) part of Dumbbell Hill locates instrument house containing time-lapse camera. Flow direction is from right to left. C. Lower Drift River valley south of DRMT. Flow from the lahars of March 26 was confined to the Rust Slough–Cannery Creek drainage where the flow width was about 2,800 m. Peak flow depth in this area was about 1 m. No flow entered the main channel of the Drift River (foreground), which remained blocked by deposits of the March 23 lahars. All photographs by C.F. Waythomas, U.S. Geological Survey, Alaska Volcano Observatory.

Figure 10. Time-lapse camera images from Dumbbell Hill of pyroclastic flow and lahar associated with eruptive event 11 and lahar 9. View is toward the west and valley width in field of view about 2 km. A. Pyroclastic flow emerging from the Drift glacier gorge and extending from left to right across piedmont lobe of the Drift glacier. Minor snowfall occurred after image was taken. B. Fresh, steaming, lahar deposits in the upper Drift River valley (shown by arrows).

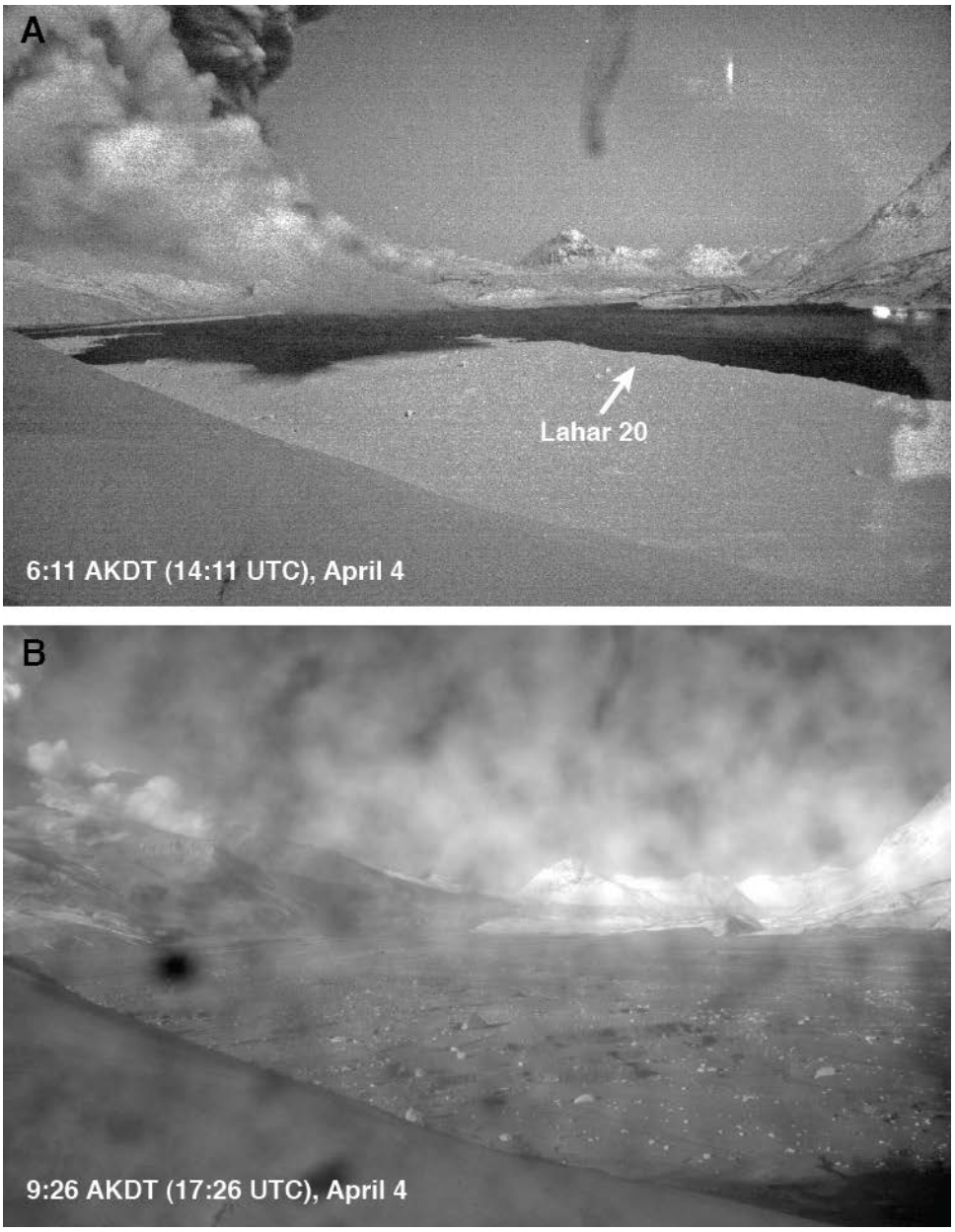

Figure 11. Time-lapse camera images from Dumbbell Hill of lahar inundating the upper Drift River valley on April 4, 2009. View is toward the west and valley width in field of view about 2 km. A. Initial surge of water at the beginning of lahar 20, 13 minutes after the start of explosive event 19. Note eruption column in upper left of image. B. Extent of inundation of the upper Drift River valley associated with lahar 20 about 3 hours after the lahar swept by Dumbbell Hill. Field of view partially obscured by ash on camera housing.

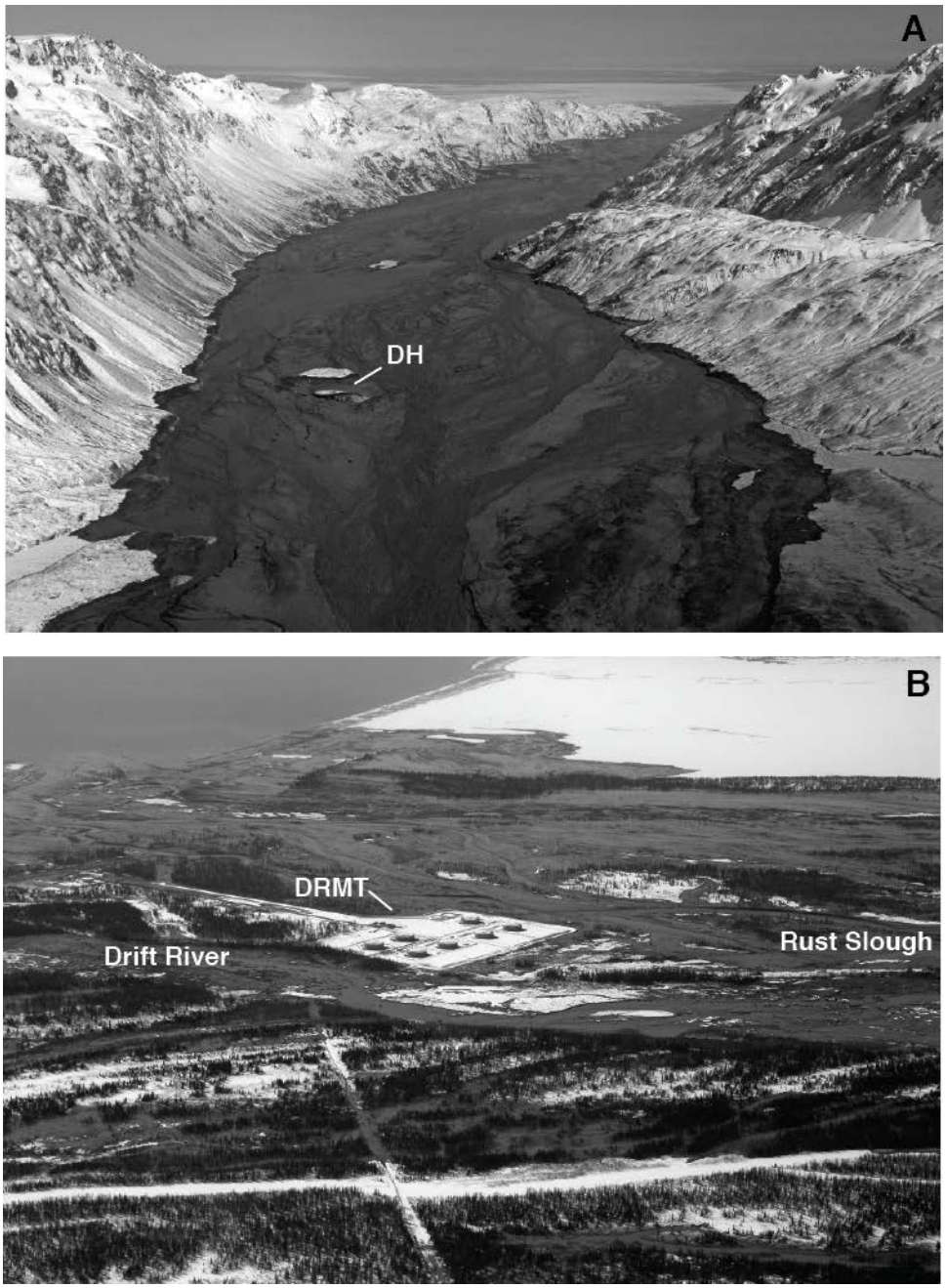

Figure 12. Inundation of the Drift River valley associated with the lahar of April 4, 2009. A. View downstream (east) of the upper Drift River in the vicinity of Dumbbell Hill (DH). The width of the channel inundated by the April 4 lahar at Dumbbell Hill is about 2 km. Flow run up on the upstream end of Dumbbell Hill about 13 m. Photograph by C.F. Waythomas, U.S. Geological Survey, Alaska Volcano Observatory, April 4, 2009. B. Extent of inundation along the lower Drift River valley in the vicinity of the DRMT. View is toward the southwest. Photograph by C.F. Waythomas, U.S. Geological Survey, Alaska Volcano Observatory.

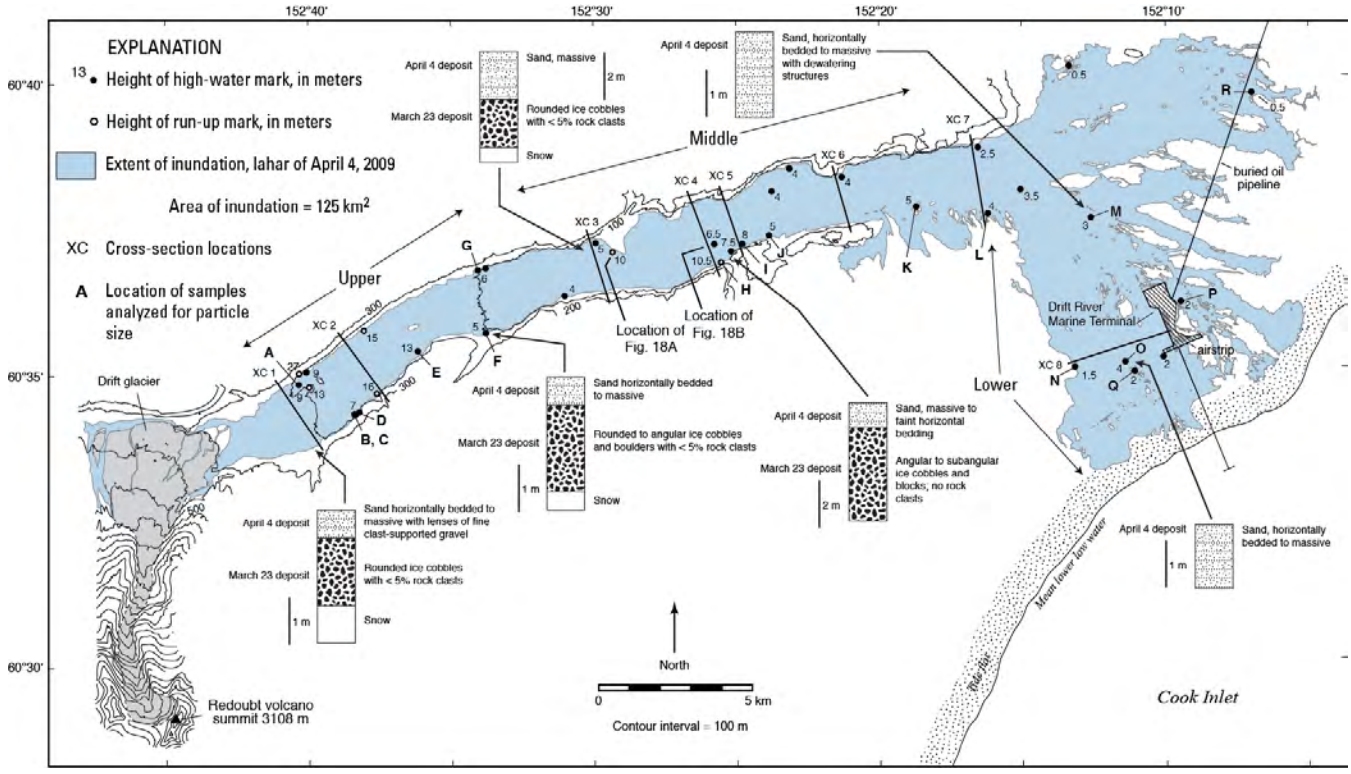

Figure 13. Map of lahar inundation associated with lahar 20 on April 4, 2009. Minimum flow depths (closed circles) and flow run up (open circles) as determined by laser rangefinder measurements of high-water marks and mud lines on trees also are shown. Location of channel cross sections used for discharge estimates, and generalized stratigraphic profiles also are shown. Locations of samples analyzed for particle-size distribution are indicated by letters A–R.

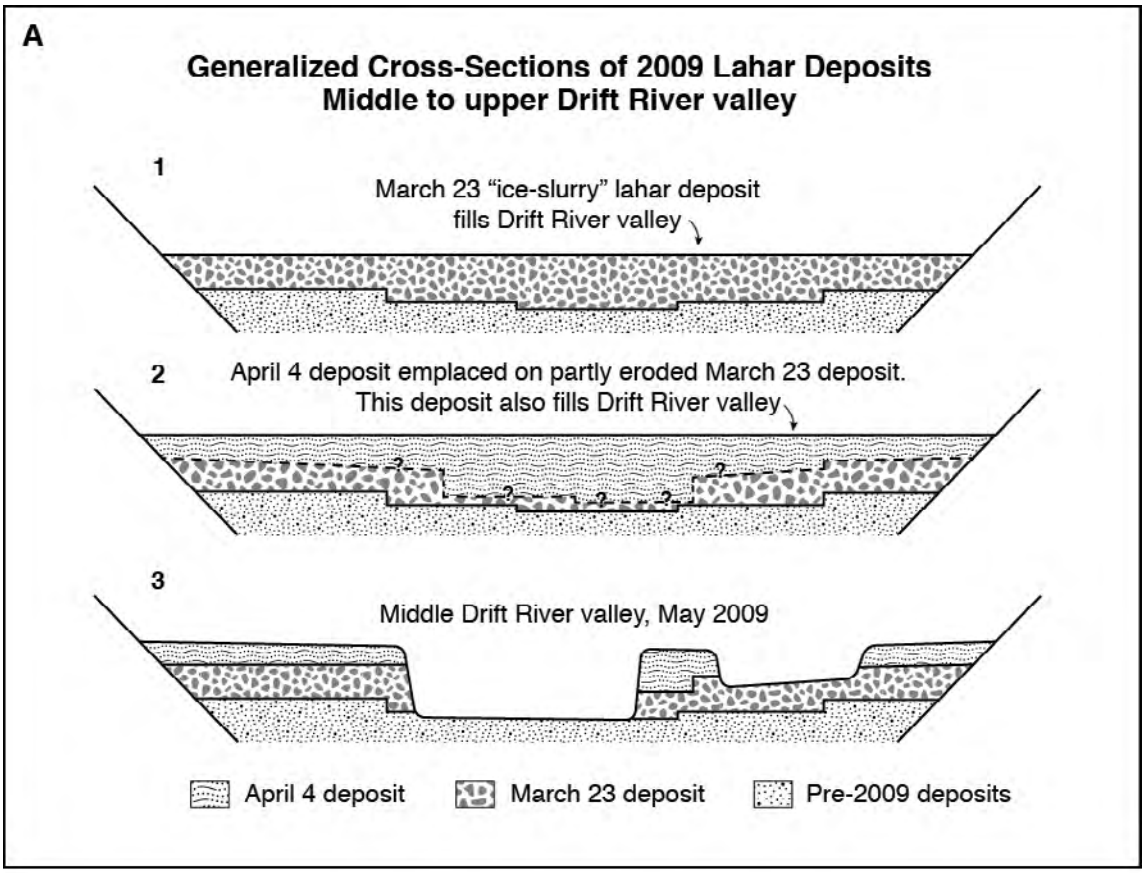

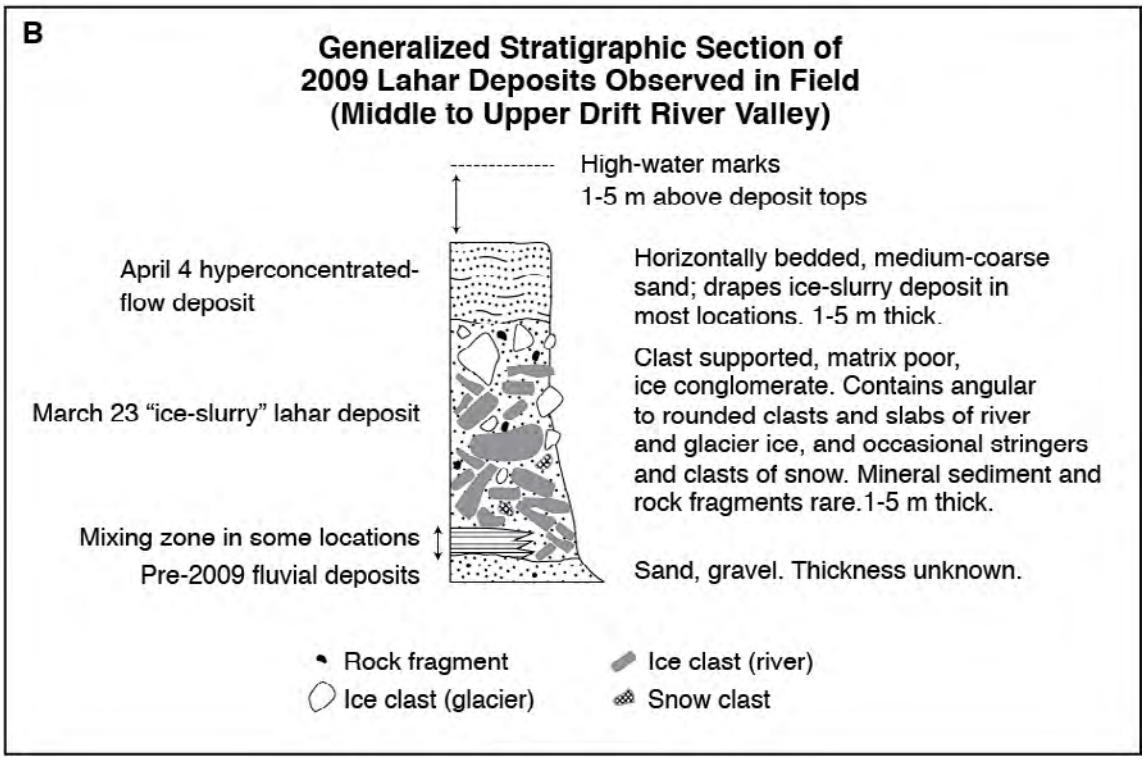

Figure 14. Generalized cross-sections (A) and stratigraphy (B) of 2009 lahar deposits in the upper to middle Drift River valley.

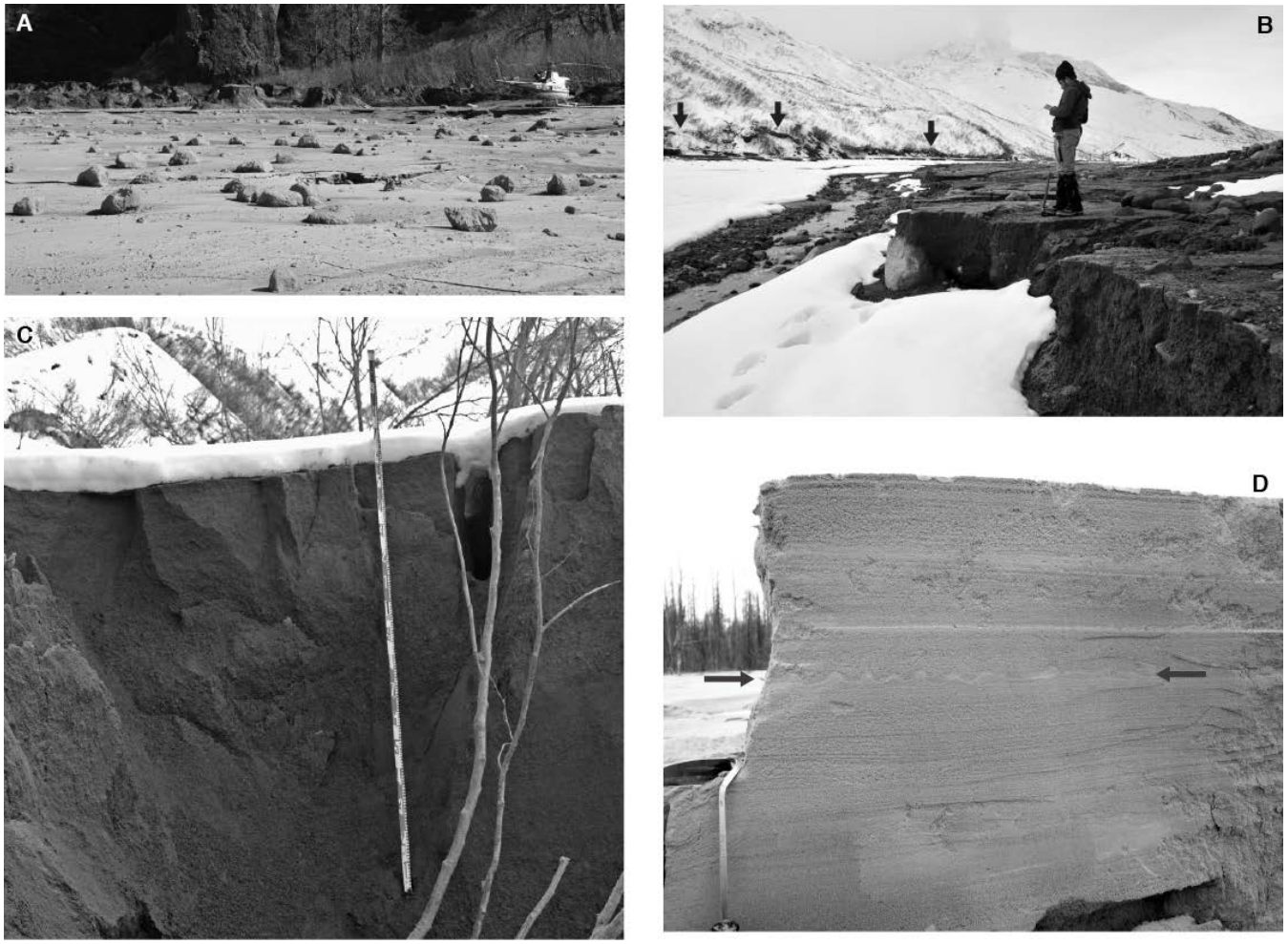

Figure 15. Photographs of April 4 lahar deposits. A. Lahar deposits in middle reach of the Drift River valley showing clasts of juvenile andesite on deposit surface that were part of the lava dome that failed on April 4. Photograph by C.F. Waythomas, U.S. Geological Survey, Alaska Volcano Observatory. B. Upper reach of the Drift River valley with Redoubt Volcano in background. Person standing on cobble and boulder gravel lahar deposits near channel axis. Arrows indicate high water mark of April 4 lahar along the southern side of valley. Photograph by C.F. Waythomas, U.S. Geological Survey, Alaska Volcano Observatory. C. Massive-to-faintly-stratified sand deposits that are characteristic of the April 4 lahar deposit. Scale in photograph is 2 m in length. Photograph by C.F. Waythomas, U.S. Geological Survey, Alaska Volcano Observatory. D. Subhorizontally stratified fine-to-medium sand deposit exposed along the lower reach of the Drift River north of the DRMT. Wavy beds shown by arrows are water-escape structures. Trenching tool in lower left for scale. Photograph by T.C. Pierson, U.S. Geological Survey, Cascades Volcano Observatory.

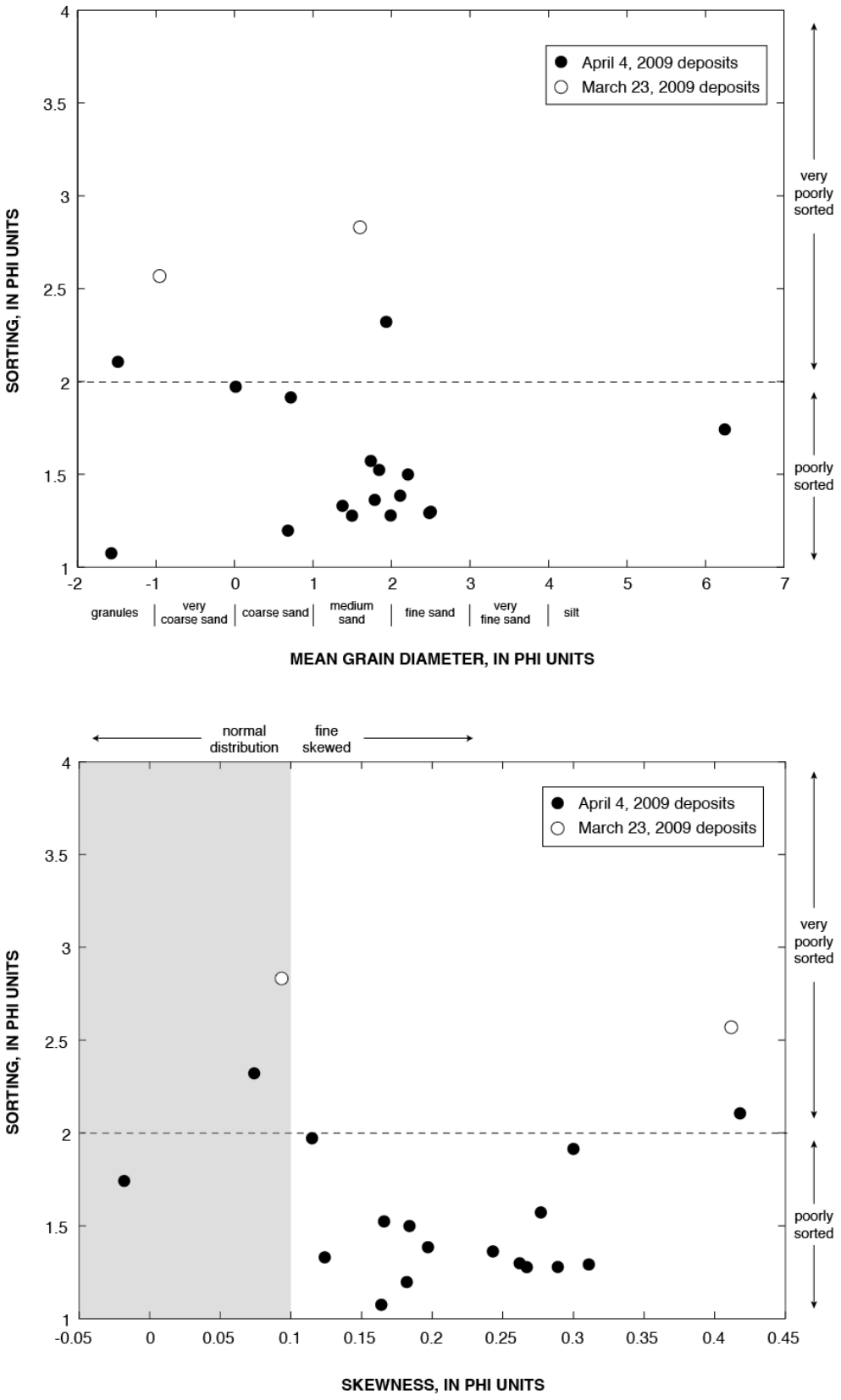

Figure 16. Plots showing sorting versus mean grain diameter, and sorting versus skewness for matrix samples of lahar deposits emplaced on March 23 and April 4, 2009.

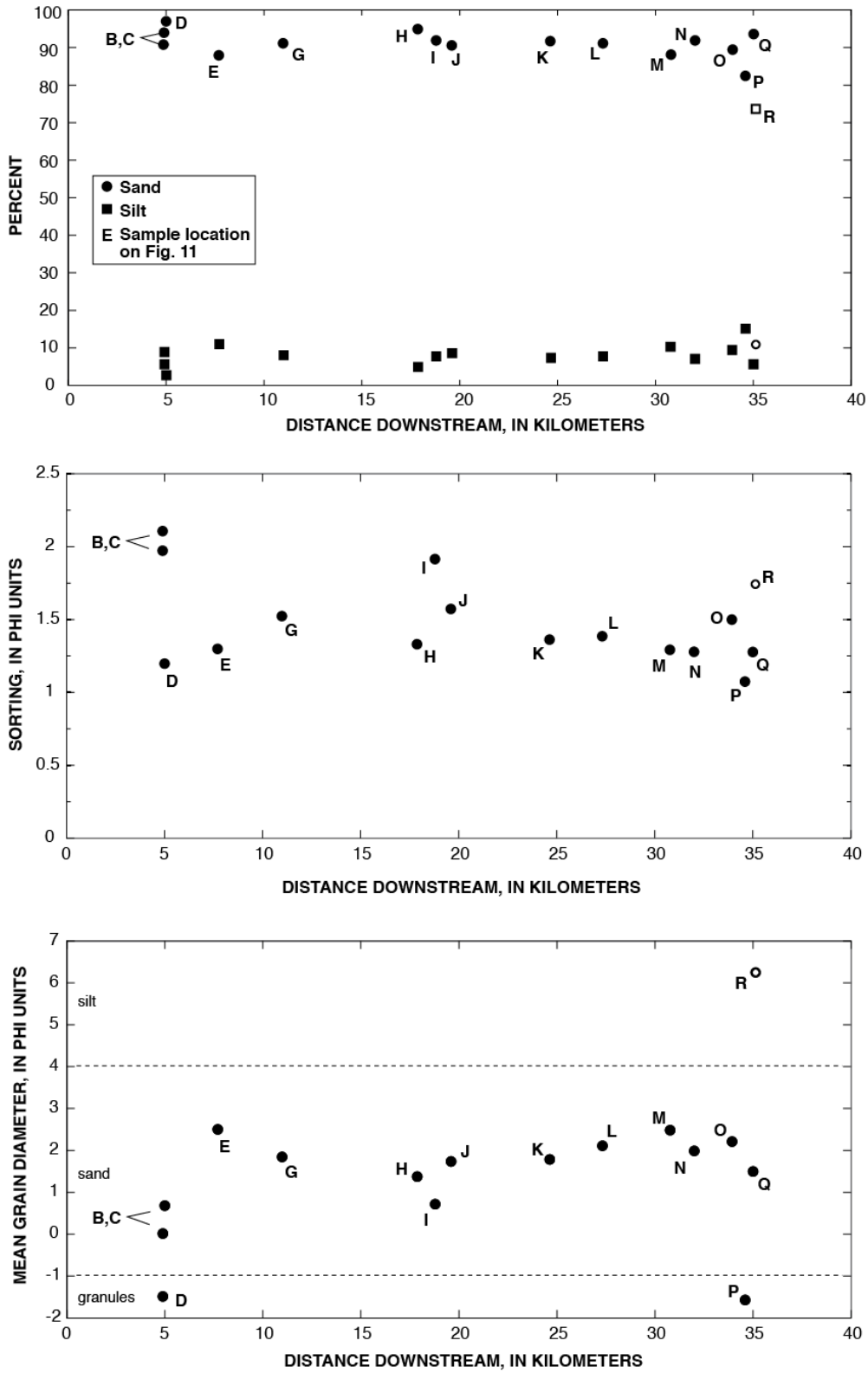

Figure 17. Percent sand, silt, sorting, and mean grain diameter of April 4, 2009 lahar deposit versus distance downstream. The sample denoted by an open symbol and labeled R was collected from the distal northern margin of the lahar deposit where the flow was tranquil. Letter labels on sample points refer to locations given in figure 13, data from sites A and F are March 23 deposits and are not included.

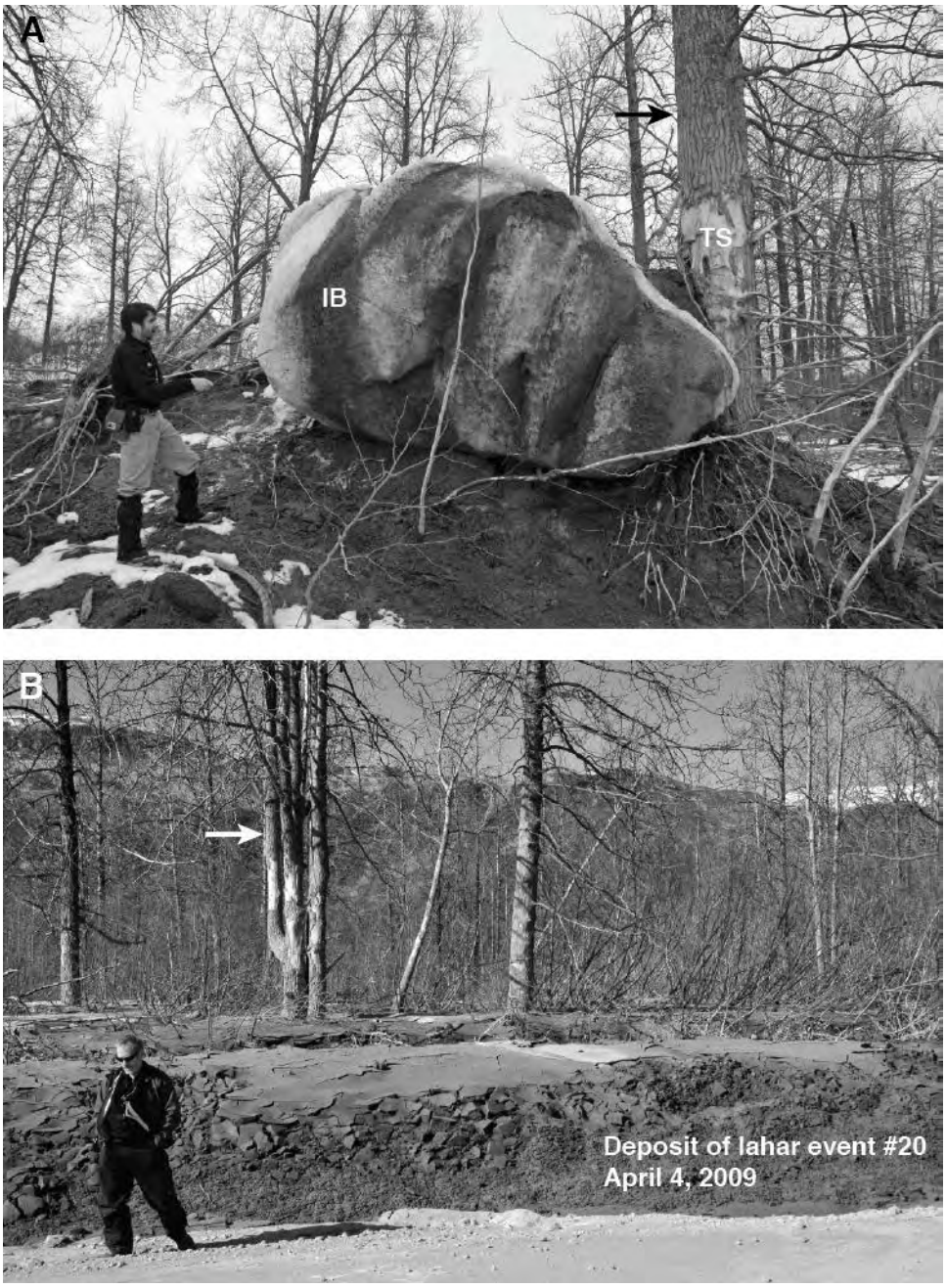

Figure 18. Examples of high water marks and deposits emplaced by lahar 20, April 4, 2009. Location of photographs are shown in figure 13. A. Arrow indicates position of mud line on tree, which records flow run up. Note tree scar (TS) probably caused by ice within the flow. The particle labeled IB is a boulder of glacier ice resting on top of a terminal moraine in the middle Drift River valley about 14 km downstream of the terminus of the Drift glacier. The top of the moraine is about 8 m above the active channel of the Drift River and was overtopped by the lahar. The highest high-water mark of lahar event 20 at this location estimated by the height of mud lines (arrow) above the active channel is 10 m. B. Sandy lahar deposits from lahar event 20 and mud line high water mark on tree (arrow) about 7 m above active channel. This site is located in the middle of the Drift River valley about 17 km downstream of the terminus of the Drift glacier. Photographs by C.F. Waythomas, U.S. Geological Survey, Alaska Volcano Observatory, April 2009.

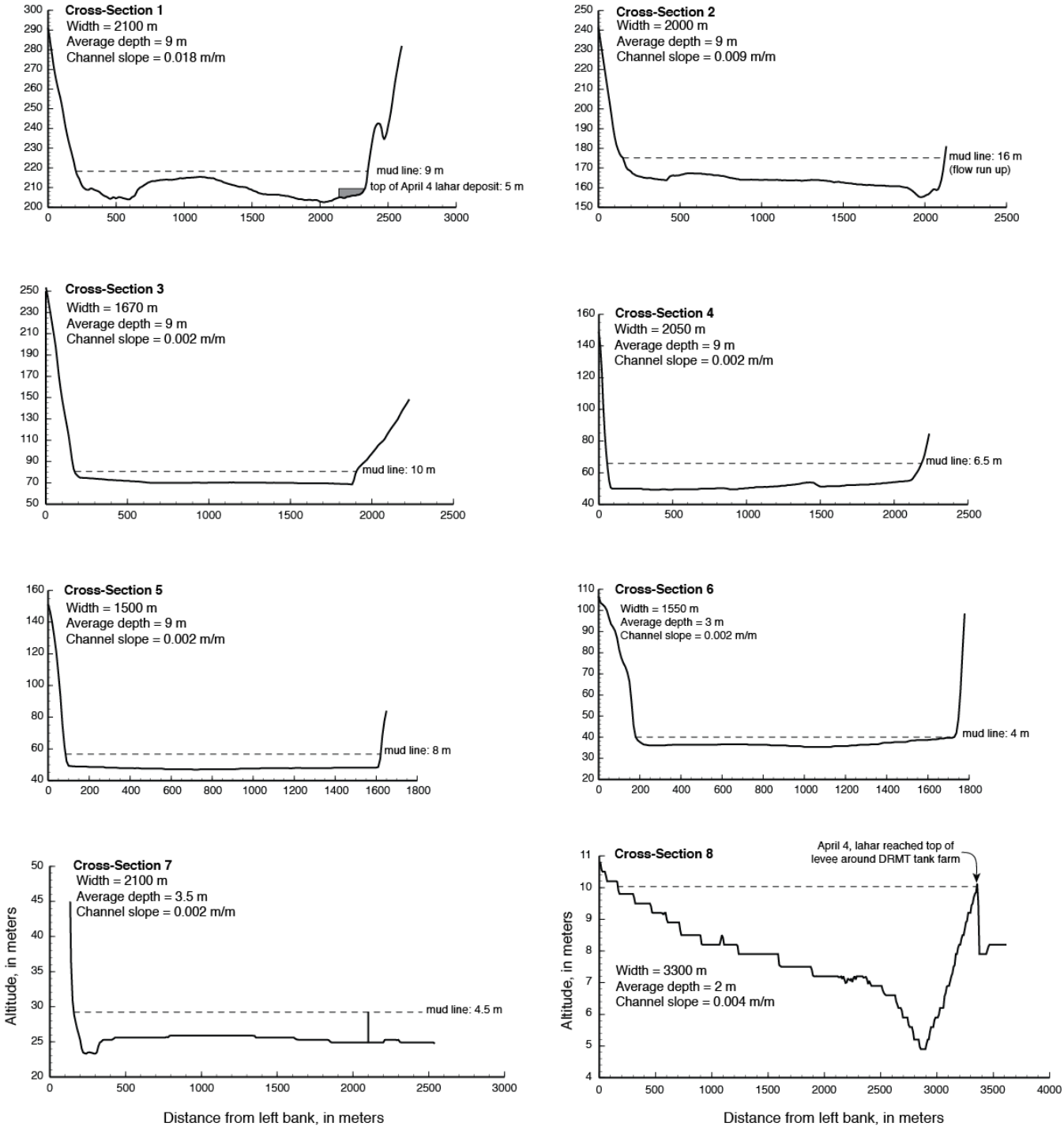

Figure 19. Channel cross sections used for estimation of average flow depth. Data used to generate cross sections were obtained from a DEM made from August 1990 topographic maps of the Drift River valley. Estimates of flow depth, shown by dashed horizontal lines, are based on measurements of the height of mud lines on trees above the nearest active channel.

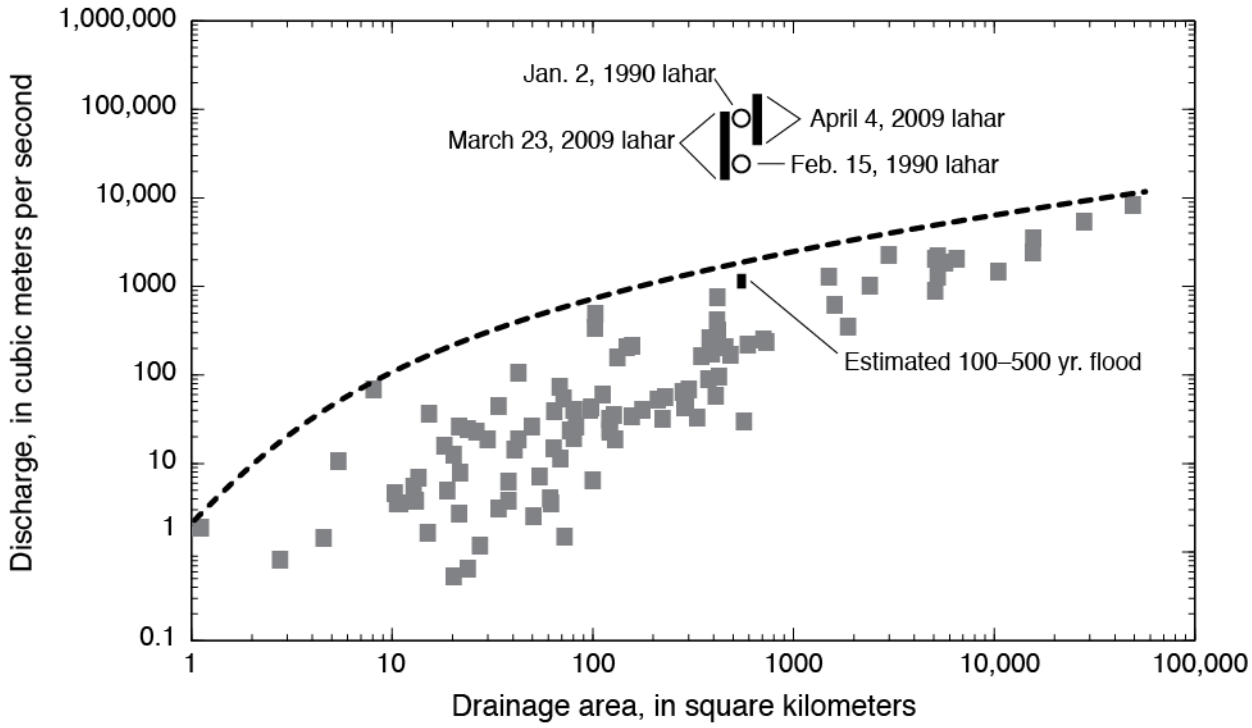

Figure 20. Peak discharge versus drainage area for meteorologically generated floods in south-central Alaska (from Jones and Fahl, 1994), compared to peak discharge of the largest lahars of the 1989–90 and 2009 eruptions of Redoubt volcano. The estimated peak discharge of the 100- and 500-year floods in the Drift River basin as determined using regional flood-frequency equations in Curran and others (2003) also is shown. The dashed line is an envelope curve indicating the largest known peak flows relative to drainage basin area.

Table 1. Estimates of ice loss[1] from the Drift glacier and the Drift River valley during 2009 eruption of Redoubt Volcano.

Time Period	Estimated ice loss, in m^3	Meltwater volume[2], in m^3	Percent of total Drift glacier ice loss	Mechanism of ice removal and comments
July 31, 2008, to March 20, 2009	$3–7 \times 10^6$	$3–6 \times 10^6$	<1	Fumarolic emissions and associated melting, magmatic heat flux
March 20–26, 2009	$0.5–1.5 \times 10^8$	$0.5–1.5 \times 10^8$	5–15	Explosive eruptive activity, near vent pyroclastic flows. Includes lahars of March 23 and 26.
March 23, 2009	Unknown	Unknown	Unknown	Snow eroded and melted by lahars of March 23 in the Drift River valley
March 27–April 4, 2009	Unknown	Unknown	Unknown	Explosive eruptive activity, near vent pyroclastic flows
April 4, 2009	$0.5–1 \times 10^8$	$0.5–1 \times 10^8$	12	Explosive eruptive activity and pyroclastic flows that swept across parts of the Drift glacier
Totals	$1–2.5 \times 10^8$	$0.9–2.3 \times 10^8$	10–25	Pre-eruption ice volume of the Drift glacier about 1×10^9 cubic meters (Trabant and Hawkins, 1997)

[1]Ice loss estimates made from analysis of satellite imagery where area of ice removal was measured in ArcMap. Ice thickness information from Trabant and Hawkins (1997). Reported values probably accurate to ± 20 percent, largely because of uncertainties associated with estimating ice thickness.

[2]Determined by multiplying total ice loss value by 0.9

Table 2. Large to moderate sized lahars of the 2009 eruption of Redoubt Volcano identified in seismic data and time-lapse camera images, March 24–30, 2009.

[Evidence: S, seismic data; TL, time-lapse camera image; V, visual observation. km^2, square kilometers]

Lahar event(s)	Date	Associated explosive event(s)	Evidence	Extent of inundation
4	March 24	6	S, TL	Northern part of the upper Drift River valley, unknown elsewhere
5, 6	March 26	7, 8	S, V	Upper and middle reaches of the Drift River valley, extent uncertain in lower reach; see figures 7 and 8. Estimated area of inundation 66 km^2.
7, 8	March 27	9, 10	S	Unknown
9	March 27	11	S, TL	Upper Drift River valley, unknown elsewhere; see figure 9
10	March 28	12	S, TL	Upper Drift River valley, unknown elsewhere
11, 12, 13, 14	March 28	13, 14, 15	S	Unknown, occurred at night
15	March 28	None	S, TL	Unknown, not associated with explosive event
16	March 28	17	S, TL	Unknown
17	March 29	18	S, TL	Extensive inundation of the upper Drift River valley, unknown elsewhere
18	March 29	None	S, TL	Minor inundation of the upper Drift River valley, not associated with explosive event
19	March 30	None	S	Unknown, not associated with explosive event

Table 3. Discharge estimates for lahar 20 of April 4, 2009.

[Locations of cross sections are shown in figure 13. km, kilometers; m, meters; v, velocity; m/s, meters per second]

Valley reach	Cross section	Distance (km)	Width (m)	Average depth (m)	Channel slope (m/m)	Discharge ($\times 10^3$ $m^3 s^{-1}$)			
						v=1m/s	v=5m/s	v=10m/s	v=15 m/s
Upper	1	3	2,100	2–5	0.018	---	---	42–105	63–157
Upper	2	5	2,000	2–5	0.009	---	---	40–100	60–150
Middle	3	14	1,670	?	0.002	---	---	---	---
Middle	4	17	2,050	?	0.002	---	---	---	---
Middle	5	18	1,500	?	0.002	---	---	---	---
Middle	6	22	1,550	?	0.002	---	---	---	---
Lower	7	26	2,100	3.5(?)	0.002	7.4	37	---	---
Lower	8	33	3,300	2	0.004	6.6	33	---	---
Lower	8	33	1,600	2	0.004	3.2	16	---	---

Table 4. Lahar volume estimates (in bold).

[km^2, kilometers; m^3, cubic meters]

Lahars	(A) Deposit area (km^2) × average deposit thickness (m) =volume (m^3)	(B) Ice-loss volume × 0.9 × bulking factor = volume (m^3)
Lahars 2 & 3 March 23	100 × 0.2–2= **2×10^7–2×10^8**	0.5–1.5 × 10^8 m^3 of ice, a portion of which was water that mobilized flow of mostly ice volume = **0.5–1.5 × 10^8 m^3**
Lahars 5 & 6 March 26	65 × 0.2–1= 1–6 × 10^7	
Lahar 20 April 4	125 × 0.5–2= **6×10^7–2.5×10^8**	0.5–1 x 10^8 m^3 ice = 0.5- 0.9 × 10^8 m^3 water × 1.5–2 = **7.5×10^7–2×10^8**

Publishing support provided by the U.S. Geological Survey
Publishing Network, Tacoma Publishing Service Center

For more information concerning the research in this report, contact the
Scientist-In-Charge, Alaska Volcano Observatory
U.S. Geological Survey
4210 University Drive
Anchorage, Alaska 99508-4650
http://www.avo.alaska.edu/